Task 2 Technical Memorandum
Analytical Modeling of the San Joaquin River

A Deliverable for
California Urban Water Agencies (CUWA)
and the
Central Valley Drinking Water Policy Work Group

Prepared by

Systech Water Resources, Inc.
1200 Mount Diablo Blvd., Suite 102
Walnut Creek, CA 94596

April 25, 2011

TABLE OF CONTENTS

List of Figures

List of Tables

1 INTRODUCTION

Background

The Watershed Analysis Risk Management Framework (WARMF) was applied to the San Joaquin River watershed from 2005-2008 to investigate the causes of dissolved oxygen impairment in the Stockton Deep Water Ship Channel ("DWSC"). Considerable scientific studies have been conducted to investigate the causes of low DO in the DWSC, including data collections, data analyses, and modeling.

In 2003, CALFED funded the directed action project for monitoring and investigations of the San Joaquin River and tributaries related to dissolved oxygen. A comprehensive field program was established to measure flow and water quality in the Upper San Joaquin River and its tributaries. Meanwhile, USGS and University of California Davis have collaborated to measure sources and transport of nutrients and algae during summer and fall of 2000 and 2001 (Kratzer et al. 2004). Jones & Stokes (2005) created a data atlas by compiling all these data into a CD to support data analysis and modeling. Task 6 of the upstream study was for the development, calibration, and application of the San Joaquin River Model.

The monitoring program performed for the upstream dissolved oxygen studies included extensive collection of data on flow, nutrients, sediment, phytoplankton, organic carbon, individual ions, and electrical conductivity. The monitoring data provided a strong basis with which to calibrate WARMF on the San Joaquin River under a variety of hydrologic conditions. The initial calibration of WARMF to the San Joaquin River is described in detail in the San Joaquin River Dissolved Oxygen TMDL Upstream Studies Task 6 Final Report (Herr, Chen, and van Werkhoven 2008).

From 2008-2010, two additional projects were undertaken in which various aspects of the San Joaquin River WARMF model were upgraded and recalibrated. As part of the Central Valley Salinity Alternatives for Long-Term Sustainability (CV-SALTS) initiative, the WARMF model domain on the east side of the San Joaquin River between Lander Avenue and Vernalis was updated. Catchment boundaries were refined to better represent drainage patterns, groundwater pumping was added as an irrigation water source, and land use classifications and associated parameters were updated. The calibration was re-evaluated and refined for all water quality parameters following the model changes as described in the Salt and Nitrate Pilot Implementation Report (Larry Walker & Associates et al, 2010). Following the CV-SALTS initiative pilot project, the Westside Salt Assessment project, initiated by the US Bureau of Reclamation, was undertaken to identify salt sources, transport and fate within the Westside region of the San Joaquin Valley. As part of this project, the WARMF model domain on the west side of the river was updated and recalibrated.

The Central Valley Drinking Water Policy Work Group is interested in evaluating the concentrations of nutrients, salt and organic carbon at drinking water intakes in the Sacramento Basin and the Sacramento / San Joaquin Delta. To determine the sources of constituents both in the present and in the future, the Work Group called for development of analytical models of the Sacramento and San Joaquin River watersheds. The analytical models would then be linked to the DSM2 model of the Delta to determine how pollutants from the upstream watersheds would impact water quality at the Delta drinking water intakes.

Because the WARMF model had already been set up and calibrated for the San Joaquin River for multiple water quality constituents, the Work Group chose to use the existing version of the model, update the catchment land use classifications and associated parameters, and then focus on the constituents of concern. The model was re-evaluated to determine the impact of model updates and the adequacy of the calibration for nutrients, TDS/EC and organic carbon.

Modeling Objective

The objective was to update and evaluate the San Joaquin River WARMF model simulations of nutrients, TDS/EC and organic carbon to suit the needs of the Drinking Water Policy Work Group. Following are the objectives of this modeling task:

1. Update catchment land use classifications and associated model parameters for the San Joaquin River WARMF model domain between Lander Avenue and Vernalis.

2. Evaluate the impact of model changes on the calibration of nutrients, TDS and EC, and organic carbon, and, if possible, improve simulation of these constituents under a variety of hydrologic conditions

   (Refine the calibration of dissolved and total organic carbon. The original calibration of WARMF did not include organic carbon as part of its focus, although it was calibrated. The simulated organic carbon under the original calibration of WARMF did not match measured winter peak concentrations at Vernalis. Simulated total organic carbon showed peaks from phytoplankton blooms in summer which were not observed in water quality data.)

3. Characterize the sources of nutrients, TDS/EC and organic carbon as they vary throughout the year and between wet and dry years.

San Joaquin River WARMF Application

The San Joaquin River WARMF application simulates point and nonpoint source pollutant loads to the San Joaquin River. Within the river, WARMF also simulates and the growth, decay, and transport processes which would ultimately impact the pollutant load to the Delta at Vernalis. The model domain was initially set with its upstream boundary at the Lander Avenue Bridge on

the San Joaquin River. The model domain was extended upstream to Friant Dam in 2008 (Herr and Chen 2008) although Lander Avenue is still used as an upstream boundary condition when simulating the lower portion of the river.

The lower San Joaquin River has three eastside tributaries (Stanislaus River, Tuolumne River, and Merced River) that drain the Sierra-Nevada western slope westward to San Joaquin River. On the west side, there are six tributaries (Hospital/Ingram Creek, Del Puerto Creek, Orestimba Creek, Los Banos Creek, Mud Slough, and Salt Slough) that drain the Diablo Coastal Range eastward to the San Joaquin River. Upstream boundary conditions for the model were initially established at monitoring locations on each of these tributaries. The land areas draining to the San Joaquin River and its tributaries between these boundaries and the Old River were included within the WARMF model domain. The model domain and catchment boundaries were subsequently altered as part of the CV-Salts and the Westside Salt Assessment Projects. During the CV-Salts Project the catchment boundaries on the east side of the San Joaquin River were updated to coincide with a groundwater model and better represent drainage patterns. However, upstream boundaries conditions on the eastside tributaries were maintained. During the Westside Salt Assessment Project, catchment boundaries on the west side of the river were altered to coincide with subregions in the WestSim groundwater model, which also largely coincide with irrigation and water district boundaries. Upper catchments above the flat valley in the foothills of the Diablo Coastal Range were added and delineated based on subbasin boundaries within the USGS National Hydrography Dataset. Upstream boundary conditions were removed so that all land area draining from the west side of the San Joaquin River between the Mendota Pool and Old River was included in the WARMF model domain. The shallow groundwater flow and nonpoint source pollution from the land areas that is simulated in WARMF is automatically added to the adjacent river segments during simulations. The map of the watershed downstream of Lander Avenue is shown in Figure 1.1 with the model domain highlighted (dark gray). White lines within the highlighted area are catchment boundaries and colored lines are water district boundaries. The Westside portion of the domain that borders the river upstream of Lander Avenue are the Salt Slough, Mud Slough and Los Banos Creek drainages, which join the San Joaquin River downstream of Lander Avenue. The model domain includes 153 river segments and 127 catchments.

WARMF is a GIS based watershed model suitable for TMDL analysis. It is a public domain model, available from US EPA website (http://www.epa.gov/athens/wwqtsc/html/warmf.html). The model is a mature model that is compatible with other watershed models contained in the EPA BASINS. The model has complete technical documentation (Chen, Herr, and Weintraub 2001) and has been peer reviewed (Keller, 2000, 2001, Driscoll, Jr. et al. 2004). The User's Manual is available (Herr et al. 2001).

WARMF simulates the watershed processes to calculate hydrology and nonpoint source loads of pollutants from various land uses (urban, native vegetation types, and agricultural areas). The input data includes the locations of agricultural diversions, daily diversions, and amount of irrigation water applied to the agriculture lands. The model simulates percolation of irrigation water through soil, evapotranspiration of water through crops, change of groundwater table, agricultural return flow, and groundwater accretion to the river reaches. The model also

simulates the nonpoint loads of pollutants due to fertilizer applications, leaching of cations and anions from the soil, and erosion of soils from land.

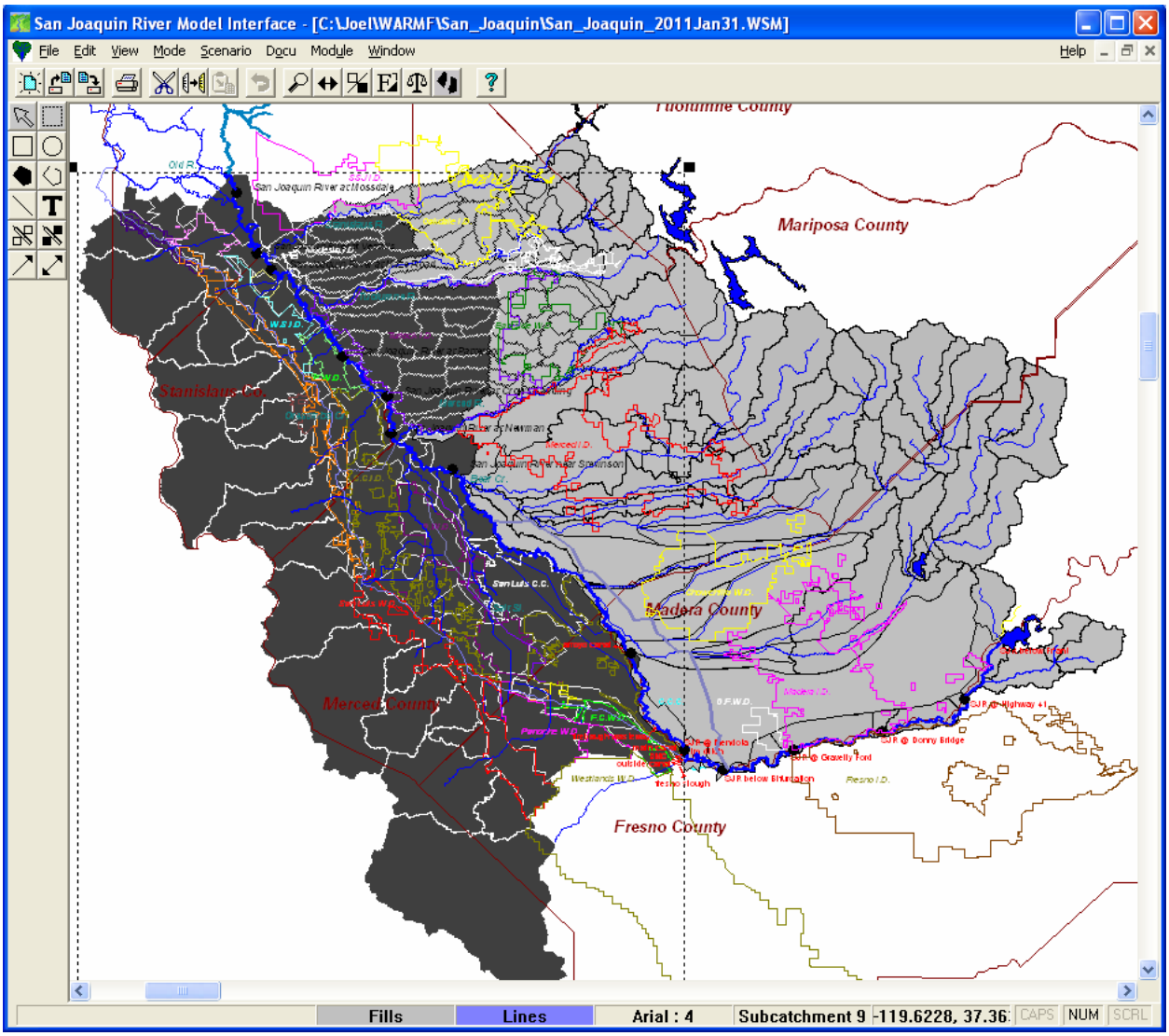

Figure 1.1 The San Joaquin River WARMF Application and Model Domain

Hydrologic Simulation

WARMF simulates hydrology based on water balance and physics of flow. It begins with precipitation on the land surface. Precipitation and irrigation water can percolate into the soil. Within the soil, water first goes to increase the moisture in each soil layer up to field capacity. Above field capacity, water percolates down to the water table, where it flows laterally out of the land catchment according to Darcy's Law. Water on the soil or within the soil is subject to evapotranspiration, which is calculated based on temperature, humidity, and season. The amount of water entering and leaving each soil layer is tracked. If more water enters the soil than leaves

it, the water table rises. If the water table reaches the surface, the soil is saturated and overland flow occurs. The overland flow is calculated by Manning's equation.

Rivers accept the subsurface and overland flow from catchments linked to them. They also receive point source discharges and flow from upstream river segments. Diversion flows are removed from river segments. The remaining water in the river is routed downstream using the kinematic wave algorithm. The channel geometry, Manning's roughness coefficient, and bed slope are used to calculate depth, velocity, and flow. The velocity is a measure of the travel time down the river, which in turn affects the water quality simulation. A thorough description of the processes simulated by WARMF is in the WARMF Technical Documentation (Chen, Herr, and Weintraub 2001).

Water Quality Simulation

The fundamental principle which guides WARMF simulation of water quality is heat and mass balance. Heat enters the soil in water from precipitation and irrigation. Heat is exchanged between catchments and the atmosphere based on the thermal conductivity of the soil. Heat in water leaving the catchments enters river segments, which combine the heat from multiple sources. As in catchments, there is thermal exchange with the atmosphere based on the difference in temperature between the water and the air. Temperature is then calculated by heat balance throughout the model.

Chemical constituents enter the model domain from atmospheric deposition and from point source discharges. They can also enter the land surface in irrigation water and fertilizer application. Chemical species move with water by percolation between soil layers, groundwater lateral flow to rivers, and surface runoff overland. Each soil layer is considered to be a mixed reactor, as is the land surface within each land use. Within the soil, cations are adsorbed to soil particles through the competitive exchange process. Anions are adsorbed to the soil using an adsorption isotherm. A dynamic equilibrium is maintained between dissolved and adsorbed phases of each ion. Reactions transform the dissolved chemical constituents within the soil. The dissolved oxygen concentration is tracked, and as DO goes to zero, anoxic reactions take place. When overland flow takes place, sediment is eroded from the catchment surface according to the modified universal soil loss equation. The sediment carries adsorbed ions (e.g. phosphate) with it to the river.

Rivers accept the water quality which comes with each source of flow. Each river segment is considered a completely mixed reactor. Ions form an equilibrium between dissolved and adsorbed to suspended sediment. Sediment can settle to the river bed and is scoured from the river bed when velocity is high enough. Chemical reactions are based on first order kinetics with their rate adjusted with a temperature correction. Algae are represented by three types: greens, blue-greens, and diatoms. Each has their own optimum growth rate, nutrient half-saturation concentrations, light saturation, optimum temperature, and temperature range for growth. At each time step, algal growth is a function of nutrient limitation, light limitation, and temperature limitation. Light penetration is a function of the algae, detritus, and total suspended sediment concentrations. Light intensity is integrated over the depth of the river segment.

Simulated Parameters

WARMF simulates a complete set of hydrologic, chemical and physical parameters as shown in Table 1.1.

Table 1.1 Parameters Simulated by WARMF

Hydrology	Flow, velocity, depth, temperature
Nutrients etc.	Ammonia, nitrate, phosphate, organic carbon (including organic nitrogen), total phosphorus, total Kjeldahl nitrogen, total nitrogen, total organic carbon, dissolved oxygen
Ions	Calcium, magnesium, potassium, sodium, sulfate, chloride, total dissolved solids, electrical conductivity, alkalinity, pH
Biological	Fecal coliform, diatoms, green algae, blue-green algae, total phytoplankton
Sediment	Clay, silt, sand, total suspended sediment, total sediment

WARMF modeled electrical conductivity (EC) in two forms. One form is an independent constituent. In this case, ECs of inflows, precipitation and irrigation water were specified in the input. The model simply tracks the EC concentration as a conservative substance. The other form was a non-conservative EC, in which WARMF modeled individual cations and anions of water. The individual ions undergo adsorption, desorption, cation exchange with soil, and reactions. The resulting concentrations of individual ions were summed for TDS. The TDS was then converted to EC by multiplying 1.667, which is a factor found to be applicable to the water in San Joaquin River.

Model Inputs

WARMF is a dynamic watershed model. It requires six categories of input data: 1) geometric dimensions of land catchments and river segments and their elevations, 2) soil characteristics of the watersheds 3) model coefficients, 4) land uses of land catchments, 5) meteorological condition, and 6) operating conditions.

The first 4 categories of data are time invariant variables, which do not change values during the model simulation. Geometric data include watershed size, average slope, and aspect, and river segment length and slope. Soil characteristics include thickness, field capacity, porosity, and hydraulic conductivity of soil layers. The model coefficients include reaction rates and their temperature correction factors. Land use data are typically imported into WARMF as shapefiles and overlaid with catchment boundaries to determine the percentage of each land use classification occurring within the catchment.

The last two categories of data (meteorological and operating conditions) are time varying. These are sometimes referred to as the driving variables. The meteorology affects the annual and seasonal variations of hydrology (i.e. dry years and wet years) and water quality (i.e. hot summers and cold winters). The operating condition includes such man-made activities as

reservoir releases, diversions, irrigation and waste discharges, which can be modified by management alternatives to improve water quality.

The daily values of driving variables are compiled and imported into the Data module of WARMF. During the simulation, the Data module automatically feeds these daily values to the model. The following sections describe the measured input data for the San Joaquin River WARMF Application.

Geometric Data

The land catchments and river segments in the San Joaquin River WARMF Model were initially delineated as part of the San Joaquin River DO TMDL Project (Herr, Chen, and van Werkhoven 2008). River segments have not been changed from the initial delineations. Changes to the catchment and river segment delineations were made during the CV-Salts Project (LWA et al, 2010) and the Westside Salt Assessment Project. Eastside catchments were delineated based on digital elevation model (DEM) data and flow patterns identified in the USGS National Hydrographic Dataset (NHD). Westside catchments were defined to correspond to water district boundaries within the valley and based on subbasins provided within the USGS National Hydrography Dataset in the foothills. Geometric dimensions and slope of catchments were calculated based on DEM data and entered into the WARMF model.

Land Use Data

The quantity, timing, and quality of surface water discharge are dependent upon the land use present within the watershed. Each land catchment simulated in the San Joaquin River watershed model was assigned various land uses on its surface based on current land use data. From the initial classifications defined in the San Joaquin River DO TMDL Project, the land use classifications in the San Joaquin River WARMF model were updated for both the CV-Salts and Westside Salt Assessment Projects.

As part of this project, a new land use dataset covering the entire model domain was provided by Newfields in the form of ESRI shapefiles for both current and future land use conditions. The new datasets contained 30 land use classes, including: Barren Land, Cotton, Deciduous Forest, Double Crop DLA, Evergreen Forest, Fallow, Farmsteads, Flowers and nursery, Grassland/Herbaceous, Marsh, Mixed Forest, Native Classes Unsegregated, Olives, Citrus & Subtropicals, Orchard, Other CAFOs, Other row crops, Paved areas, Perennial forages, Perennial Forages DLA, Rice, Sewage plant including ponds, Shrub/Scrub, Urban Commercial, Urban Industrial, Urban landscape, Urban residential, Vines, Warm season cereals/forages, Water, and Winter grains & safflower. These 30 classes were merged with existing land use classifications (defined in the model as part of the Westside Salt Assessment Project), resulting in a total of 41 land use categories defined in WARMF. The additional 11 land use classes that remained in WARMF from previous projects include Almonds, Pistachios, Alfalfa, Grain, Corn, Tomatoes, Sugar Beets, Potatoes, Onions and Garlic, Cucurbits, and Beans.

Based on the new land use dataset, percentages of each WARMF catchment's area covered by each land use class were defined in WARMF. In the version of the model setup for this project,

the 11 classifications carried over from previous projects have zero percentage of the catchment area.

Meteorology Data

Meteorology data from the years 1997-2007 was collected and imported into WARMF for the initial model setup during the San Joaquin River DO TMDL Project (Herr, Chen, and van Werkhoven 2008). When meteorology stations are imported into WARMF, the nearest station is assigned to each catchment and a precipitation weighting factor and temperature lapse rate are automatically calculated to account for regional climate variation. After changes were made to the catchment delineations in both the CV-Salts and Westside Salt Assessment projects, meteorology stations were re-imported to recalculate the precipitation weighting factors and temperature lapse rates for the entire WARMF domain.

For this project additional meteorology data were collected from the CIMIS and CDEC databases in order to extend the meteorology database back in time so that the model could be run for an earlier period (1975-1991). Quality control was performed to remove suspicious or inconsistent data. For years in which no data were available, values were estimated from the nearest station with recorded data and adjusted based on relative differences in long-term climatic averages. The meteorology stations used for the San Joaquin WARMF model, the dates of acceptable available data, and the dates of removed (poor quality) data are listed in Table 1.2. The locations of the stations are shown in Figure 1.2.

Table 1.2 Meteorology Stations Used in the San Joaquin River WARMF Application

Station name	Source	Dates of acceptable data	Dates removed
Firebaugh	CIMIS #7	5/1996 – present	9/1982 – 11/1989
Fresno	CIMIS #80	10/1988 – present	None
Friant	CDEC FRT	2/1989 – present	None
Hensley	CDEC HID	1/1988 – present	None
Kesterson	CIMIS #92	10/1989 – present	None
Los Banos	CIMIS #56	7/1988 – present	None
Madera	CIMIS #145	5/1998 – present	None
Manteca	CIMIS #70	11/1987 – present	None
Merced	CIMIS #148	1/1999 – present	None
Modesto	CIMIS #71	7/1987 – present	None
Panoche	CIMIS #124	8/1995 – present	11/19/1995, 8/11/1995

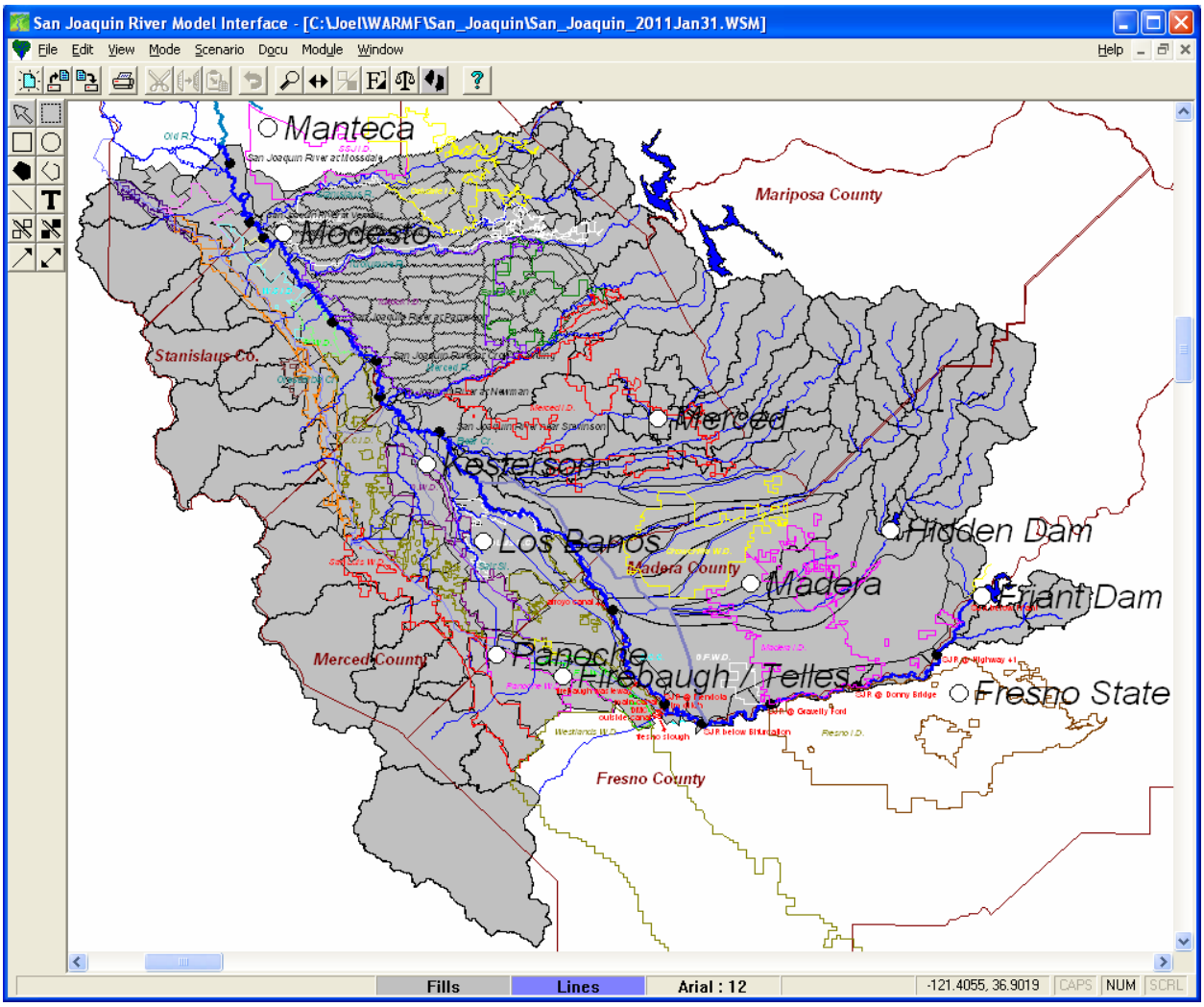

Figure 1.2 Locations of Meteorology Stations in the San Joaquin River Watershed

Air Quality and Rain Chemistry Data

Air quality and rain chemistry data were initially processed as part of the San Joaquin River DO TMDL Project (Herr, Chen, and van Werkhoven 2008). Air quality data were used to calculate the dry deposition of atmospheric ammonia, nitrate, and other constituents to the land and canopy surfaces. Weekly air quality data were obtained from the US EPA's Clean Air Status and Trends Network (CASTNET) site at Yosemite National Park.

Rain chemistry data was used to calculate wet deposition falling onto each of the land catchments. Data for rain chemistry were compiled from two National Atmospheric Deposition Program (NADP) sites in the vicinity of the San Joaquin River drainage basin: Davis and Yosemite National Park. Data from these stations were entered on a weekly basis for input to the WARMF model. As part of this project, air quality and rain chemistry data were extrapolated back in time based on average monthly mean values in order to run the model for an earlier time period (1975-1991).

Boundary River Inflows

Boundary river inflows are external inputs to the model. These inputs are treated like "point sources", with data for inflow quantity and associated water quality. Boundary inflows in the preexisting San Joaquin River WARMF application included three east side tributaries (Stanislaus River, Tuolumne River, Merced River), the San Joaquin River at Lander Avenue near Stevinson (Bear Creek), seven west side tributaries (Salt Slough, Mud Slough, Los Banos Creek, Orestimba Creek, Del Puerto Creek, Ingram Creek, and Hospital Creek), and the inflow to the Delta-Mendota Canal (DMC). During the Westside Salt Assessment Project, the contributing catchment areas for the seven Westside tributaries were added to the active model domain and therefore the seven Westside tributary inflows were removed from the model. In addition, two Westside inflows were added to better track water quality and account for sources correctly – inflow to Mendota Pool from James Bypass (Fresno Slough) and inflow to the DMC below O'Neill Forebay. The latter inflow is not truly a model "boundary," but was necessary due to the fact that San Luis Reservoir and O'Neill Forebay are not included in the WARMF model. However exchange of water between the DMC and O'Neill Forebay may significantly alter the water quality in the DMC below the exchange point. Thus water quality in the lower portion of the DMC was assigned based on water quality data from DMC Checks 20 and 21. The lower DMC flow was determined based on inflow into the upper portion, deliveries above O'Neill Forebay, and exchanges (spills or pumping) at the O'Neill Forebay.

The final seven boundary river inflows in the San Joaquin River WARMF Application and their sources of flow and water quality data are listed in Table 1.3. As part of this project, additional historical data were collected to extend the boundary inflows back in time and enable running the model for an earlier time period (1975-1991).

Table 1.3 Data Sources for Boundary River Inflows

Boundary Inflow	Source of Flow Data
Stanislaus River at Ripon	USGS 11303000
Tuolumne River at Modesto	USGS 11290000
Merced River at Stevinson	USGS 11272500 and CDEC MST
San Joaquin River at Lander Ave.	CDEC SJS
Upper Delta Mendota Canal	DMC Headworks, CDEC-DWR
Lower Delta Mendota Canal	Upper DMC outflow, USBR CVO Table 24 - ONeill Pumping
Mendota Pool from Fresno Slough	USGS 11253500

Point Source Discharge Data

Two major point source discharges exist within the active San Joaquin River WARMF model domain – the Modesto Water Quality Control Facility and the City of Turlock Waste Water Treatment Plant. Flow and water quality data were defined for these two locations using data in the EPA National Pollutant Discharge Elimination System (NPDES) database. Five smaller facilities exist within the model domain shown in . Permitted dairy dischargers are simulated in WARMF using land application rates rather than as point source inputs. Point sources included

in WARMF are shown in Table 1.4. Twenty other point source discharges shown in Table 1.5 were defined within WARMF as part of previous projects, but are located outside of the active model domain boundary (see Larry Walker Associates et al, 2010).

Table 1.4 Point Sources Included in WARMF

Facility	County	Flow, MGD	Discharge
Modesto WQCF	Stanislaus	19.2	Land, surface water
City of Turlock	Stanislaus	11.3	Surface water
Bronco Wine Company	Stanislaus	no data	
AG 45 Inc.	Stanislaus	1.0	Land
City of Ceres	Stanislaus	1.8	Land
Darling International	Stanislaus	no data	
Hilmar Cheese	Stanislaus	0.7	Land

Table 1.5 Point Sources Outside Active WARMF Model Domain

Facility	County	Flow, MGD
7 11 Materials	Stanislaus	0.74
Chukchansi Gold Resort & Casino	Madera	no data
California Department of Fish & Game San Joaquin Hatchery	Fresno	no data
Planada CSD WWTF	Merced	0.56
City of Atwater	Merced	4.64
City of Merced WWTF	Merced	13.15
General Electric Company	Merced	no data
Fresno Metropolitan FCD	Fresno	no data
North Fresno WWTF	Fresno	no data
AG 45	Stanislaus	1.55
City of Hilmar	Stanislaus	1.24
City of Hughson	Stanislaus	1.24
City of Oakdale	Stanislaus	3.71
City of Riverbank	Stanislaus	11.61
City of Waterford	Stanislaus	1.55
Conagra Grocery	Stanislaus	no data
Foster Farms	Stanislaus	5.88
Hershey Foods	Stanislaus	6.96
Hughson Nut Company	Stanislaus	2.01
Santa Fe Aggregates	Stanislaus	1.55

Fertilizer Application Data

WARMF allows for monthly land application loading inputs for each land use. Land application represents any loading to the land surface which does not come from the atmosphere. It includes fertilizer in agricultural and urban land uses and disposal of animal waste from dairies and other confined feeding operations. The application rates used were estimated by NewFields based on agricultural practices in the San Joaquin River watershed. A detailed explanation of the methods

used to estimate land application rates will be provided by NewFields in a separate document. The nitrogen, sulfate and phosphorus application rates used in WARMF are shown in The application rates in dairy land use classes (Perennial Forages DLA and Double Crop CLA) varied by catchment. Thus, the range of application for each nutrient is listed in Table 1.6 for these two land use classifications.

Table 1.6 Land Application Rates

Land Use	Ammonia Application Rate, lbs N/acre/yr	Nitrate Application Rate, lbs N/acre/yr	Sulfate Application Rate, lbs/acre/yr	Phosphate Application Rate, lbs P/acre/yr	Application Months
Grassland/Herbaceous	0	0	0	0	0
Evergreen Forest	0	0	0	0	0
Deciduous Forest	0	0	0	0	0
Mixed Forest	0	0	0	0	0
Shrub/Scrub	0	0	0	0	0
Other Native classes	0	0	0	0	0
Barren Land	0	0	0	0	0
Marsh	0	0	0	0	0
Orchard	240	0	785.56	24	4-10
Almonds	240	0	785.56	24	4-10
Pistachios	240	0	785.56	24	4-10
Perennial forages	120	0	392.78	12	3-11
Alfalfa	120	0	392.78	12	3-11
Grain	198	0	648.09	19.8	3-5
Winter grains and safflower	198	0	648.09	19.8	3-5
Corn	300	0	981.95	30	4-8
Warm season cereals and forages	300	0	981.95	30	4-8
Tomatoes	194.4	21.6	558.91	21.6	5-9
Sugar Beets	194.4	21.6	558.91	21.6	5-9
Potatoes	194.4	21.6	558.91	21.6	5-9
Onions and Garlic	194.4	21.6	558.91	21.6	5-9
Cucurbits	194.4	21.6	558.91	21.6	5-9
Beans	194.4	21.6	558.91	21.6	5-9
Other row crops	194.4	21.6	558.91	21.6	5-9
Cotton	216	0	707.01	21.6	4-10
Flowers and nursery	120	120	0	24	3-10
Olives, citrus, and subtropicals	318	0	1040.9	31.8	3-10
Rice	110	0	360.05	11	5-9
Vines	105.6	26.4	251.05	13.2	4-9
Other CAFOs					
Perennial forages Dairy Land App.	475 - 1963	25 - 103	1465 - 6054	50 - 207	3-11
Double Crop Dairy Land Application	475 - 3111	25 - 164	1465 - 9595	50 - 327	3-9
Farmsteads	268.8	67.2	639.03	33.6	3-11
Fallow					
Urban residential	11.2	2.8	26.9	1.25	3-11
Urban landscape and open space	31.4	7.84	78.7	1.25	3-11
Urban commercial	2.4	0.6	4.2	1.25	3-11
Urban industrial	1.2	0.3	1.15	1.25	3-11
Sewage treatment plant	0	0	0	0	0
Paved areas	0	0	0	0	0
Water	0	0	0	0	0

Irrigation Water

Due to the changes in land use classifications that were made for this project, it was also necessary to update the allocation of irrigation water. The San Joaquin River WARMF model domain includes 28 irrigation or water districts (7 on the Eastside and 21 on the Westside), 4 cities, and several unincorporated areas that receive irrigation water to support agriculture. In addition, the Westside region includes 10 units of state or federal refuges that receive irrigation water to maintain seasonal wetlands. The water sources for these districts, cities and refuges are diversions from the San Joaquin River, Stanislaus River, Tuolumne River, DMC, San Luis Canal, and Mendota Pool, as well as pumped groundwater. Table 1.7 lists the mean annual deliveries (WY 2000-2007) for diversions and the water source. DMC diversions with outflow points above O'Neill Forebay (canal mile 70.01) are specified as "Upper DMC" diversions, while those with outflow points below the Forebay are "Lower DMC" diversions.

Table 1.7 Irrigation Diversions and Sources

Water Source	Receiving Entity	Mean Annual Delivery (acre-ft/yr)
Stanislaus R.	Oakdale ID	276655
Stanislaus R.	South San Joaquin ID	221324
Tuolumne R.	Turlock ID	542964
Tuolumne R.	Modesto ID	284166
San Joaquin R.	River Junction Recl. District #2064	11502
San Joaquin R.	Freitas Unit - San Luis NWA	1511
San Joaquin R.	China Island Unit - N. Grasslands WA	7920
San Joaquin R.	Unincorporated Area -Subcatchment 955	6155
San Joaquin R.	City of Crows Landing	1350
San Joaquin R.	Patterson WD	40765
San Joaquin R.	Unincorporated Area -Subcatchment 188	4574
San Joaquin R.	West Stanislaus WD	13179
San Joaquin R.	Subcatchment 188 & West Stanislaus ID	11010
San Joaquin R.	Byron Bethany ID	5752
San Joaquin R.	El Solyo WD	22004
San Joaquin R.	Banta Carbona ID	37770
Upper DMC	Banta-Carbona ID	1964
Upper DMC	Byron Bethany ID	3277
Upper DMC	CCID Above Check 13	15245
Upper DMC	Centinella WD	41
Upper DMC	City of Tracy	8242
Upper DMC	Del Puerto WD	80462
Upper DMC	Patterson WD	5947
Upper DMC	West Stanislaus WD	32679
Upper DMC	Westside ID	825
Upper DMC	Grasslands WD (Volta)	37186
Upper DMC	Kesterson NWA (Volta)	4085
Upper DMC	Volta WMA	7911
Lower DMC	Broadview WD	6487
Lower DMC	CCID Below Check 13	77727

Water Source	Receiving Entity	Mean Annual Delivery (acre-ft/yr)
Lower DMC	Eagle Field WD	2446
Lower DMC	Firebaugh Canal Co.	26652
Lower DMC	Mercy Springs WD	1478
Lower DMC	Oro Loma WD	1088
Lower DMC	Panoche WD	6375
Lower DMC	San Luis WD	11158
Lower DMC	Widren WD	66
Lower DMC	China Island Unit - N. Grasslands WA	2976
Lower DMC	Freitas Unit - San Luis NWA	3472
Lower DMC	Grasslands WD (76.05L)	60249
Lower DMC	Kesterson NWA (76.05L)	1651
Lower DMC	Los Banos WMA	5135
Lower DMC	Salt Slough Unit - N. Grasslands WA	4718
Mendota Pool	CCID	421013
Mendota Pool	Columbia Canal Co.	53535
Mendota Pool	Firebaugh Canal Co.	33564
Mendota Pool	San Luis Canal Co.	138846
Mendota Pool	China Island Unit - N. Grasslands WA	4821
Mendota Pool	Freitas Unit - San Luis NWA	5600
Mendota Pool	Grasslands WD	129549
Mendota Pool	Kesterson NWA	2424
Mendota Pool	Los Banos WMA	15565
Mendota Pool	Salt Slough Unit - N. Grasslands WA	6513
Mendota Pool	San Luis Unit – San Luis NWA	31646
San Luis Canal	Pacheco WD	7633
San Luis Canal	Panoche WD	52175
San Luis Canal	San Luis WD	65735
O'Neill Forebay	San Luis WD	9179

The diversions from the Stanislaus River, DMC, Mendota Pool and San Joaquin River are diverted from river and canal segments that are included in the WARMF model domain and are thus simulated dynamically. WARMF diverts the quantity of irrigation waters from their respective diversion points and uses the simulated water quality for the irrigation water. A few districts use irrigation water diverted from river and canal segments that are not a part of the active WARMF model domain, namely from the upper Tuolumne River, San Luis Canal, O'Neill Forebay, and California Aqueduct. For these diversions, the flow and water quality were defined directly in a WARMF point source file. The San Luis Canal and O'Neill Forebay delivery quantities were obtained from USBR Central Valley Operations (CVO) tables with water quality assumed to be the same as the DMC.along with DMC water quality, since no water quality data for the canal and forebay were readily available. The California Aqueduct diversion was included to supply irrigation water to Oak Flat Water District, which has a contract with the State Water Project. The contracted annual delivery amount of 5700 acre-ft/year was used for the delivery quantity and water quality was assumed to be the same as the DMC.along with DMC.

The diversion data was collected and processed as part of previous projects (San Joaquin River DO TMDL, CV-SALTS, and Westside Salt Assessment projects). Since land use changed during this project, the allocation of irrigation water to each new WARMF subcatchment was updated. For agricultural areas (versus wildlife refuge areas), irrigation allocation involved both the analysis of the irrigation demand within each catchment, and the evaluation of total delivery quantities. The quantity of irrigation demand within each land catchment was calculated using a geographic information system (GIS). In the GIS, an intersection between layers representing the WARMF catchments and the irrigation district boundaries was created. The resulting layer was then employed to query a land use dataset to determine the land use distribution within each irrigation district present within each of the WARMF catchments. The calculated areas of each irrigated land use were used to estimate the demand for irrigation water within each of the WARMF catchments. Irrigation requirements for various land uses and CIMIS Evapotranspiration Zones (provided by NewFields) are shown in .

Table 1.8 Applied Irrigation Rates (feet/year)

Land Use Class	**CIMIS Evapotranspiration Zone[1]**				
	10	**11**	**12**	**14**	**15**
Cotton	3.2	N/A	4.2	4.3	4.6
Double Crop DLA	N/A	N/A	4.6	4.2	4.5
Farmsteads	3.4	4.4	5.3	5.4	6
Flowers and nursery	N/A	N/A	2.6	2.7	3
Olives, citrus, and subtropicals	N/A	2.2	2.6	2.7	3
Orchard	2.5	3.2	3.7	3.8	4
Other row crops	3	N/A	3.7	3.9	4
Perennial forages	3.1	4.1	4.9	5	5.6
Perennial forages DLA	N/A	N/A	4.9	5	5.6
Rice	N/A	N/A	3.9	N/A	4.2
Urban commercial	N/A	2.4	2.9	2.9	3.2
Urban industrial	1.8	2.4	2.9	2.9	3.2
Urban landscape and open space	2.9	3.8	4.6	4.7	5.2
Urban residential	3.4	4.4	5.3	5.4	6
Vines	1.5	1.9	2.2	2.3	2.5
Warm season cereals and forages	2.9	3.3	3.6	3.7	3.9
Winter grains and safflower	0.2	0.6	1.2	1.2	1.6

[1]Values of N/A represent combinations of land use class and evapotranspiration zone that do not exist within the San Joaquin River WARMF model domain

The available surface water for a given catchment was identified based on delivery data for the corresponding receiving entity (irrigation district, city or refuge). If more than one catchment corresponded to a given entity (e.g. Turlock, Modesto, Central CA Irrigation Districts (CCID)), the diversion for that entity was divided in proportion to the demand within each catchment. In Eastside catchments and in Westside catchments covering the CCID area, groundwater pumping information was available to estimate the total amount of groundwater applied as irrigation. In Westside catchments where groundwater pumping information was not available, groundwater usage was assumed to be the additional water quantity necessary to meet the irrigation demand after all available surface water was applied.

For refuge (wetland management) areas, determination of applied irrigation water relied entirely on the calculated amount of surface water delivered (from CVO Tables), since no "demand" could be calculated for these areas. If more than one catchment corresponded to a given refuge or diversion, the diversion for that refuge was divided in proportion to the relative area of grassland contained in each catchment.

The monthly pattern and year-to-year variation of surface water applied for irrigation was assumed to be proportional to the patterns in the associated delivery tables. The diversions typically follow a seasonal pattern: near zero before February, increasing until midsummer, and then decreasing until November. In agricultural catchments, the intra-annual variability in total deliveries is generally low. For groundwater applied to agricultural areas, average monthly patterns from the Modesto and Turlock Irrigation Districts (Eastside), and from CVO diversions (Westside) were used.

2 MODEL CALIBRATION

Procedure

Given meteorological and operational data, the San Joaquin River Model made predictions for stream flow and water quality at various river segments. At locations where monitoring data was collected, the model predictions should generally match the measured stream flow and water quality. Initially, some model coefficients, such as physical properties of the watershed, are known. Other coefficients are left at default or typical literature values. When the model was first setup and updated in past projects, the model predictions made did not necessarily match the observed values. Model calibration was performed in phases throughout multiple projects by adjusting model coefficients and input assumptions within reasonable ranges to improve the match between model predictions and observed data.

The model predictions and observed data were compared graphically. In the graph, the time series of model predictions were plotted in a curve on top of measured data. If the observed values fell on top of the curve, the match could be determined as good or poor by visual inspection.

The model predictions and observed data were also compared statistically. The differences between the predicted and observed values are errors. The magnitudes of the errors were calculated in the statistical terms of relative error, absolute error, root mean square error, and correlation coefficient. The relative (E_r) and absolute (E_a) errors are the primary statistics used in model calibration and are described as follows:

$$E_r = \frac{\sum (simulated - observed)}{n}$$

$$E_a = \frac{\sum |simulated - observed|}{n}$$

The error of each instance where there are both simulation results and observed data is the simulated minus the observed. The relative error cancels out errors greater than and less than observed and is thus a measure of model accuracy or bias. The absolute error measures model precision. Both can be expressed as a percent by dividing by the average observed value. Calibration goals for flow and conservative substances are less than 10% relative error and less than 20% absolute error. For non-conservative substances, an absolute error of 30% is more realistic. Because total suspended sediment is very difficult to model with precision, higher absolute error is expected while calibration can realistically achieve a good relative error.

Both graphical and statistical comparisons were made with WARMF. WARMF has a scenario manager, where each scenario is a set of model input coefficients and corresponding simulation

results. Scenario 1 may be used to represent a set of numerical values of model coefficients used in the simulation. Scenario 2 may be used to represent a second set of modified model coefficients used in the simulation. After the simulation, WARMF can plot the observed data as well as the model predictions for both scenarios on the same graph. By visual inspection, it is relatively easy to see whether the changes to model coefficients improve the match.

Likewise, WARMF calculates the values of various error terms for the model predictions. The comparison of the numerical values of errors for two scenarios can lead the user to adjust the model coefficients in the right way to reduce the errors.

Model calibration followed a logical sequence. Hydrological calibration was performed first, because an accurate flow simulation is a pre-requisite for accurate water quality simulation. The calibrations for temperature and conservative substances were performed before the calibration of nutrients (phosphate, ammonia, and nitrate), algae and dissolved oxygen concentrations.

Only a few model coefficients were adjusted for each calibration. For hydrological calibration, the boundary river inflows were checked for accuracy. Evapotranspiration coefficients, field capacity, saturated moisture, and hydraulic conductivity are then adjusted so that the simulated agricultural return flow and groundwater accretion could account for flow changes between the monitoring stations. For water quality calibration, the growth rate and half saturation constants of algae have been measured in the field program. The measured values were used to replace the default values contained in WARMF.

After submission of the Calibration Report (Herr and Chen 2006a), riparian diversions were added to WARMF in response to feedback from the Modesto and Turlock Irrigation Districts. A review of the model performed by Flow Science (List and Paulsen 2008) recommended several improvements to the calibration. The calibration was modified in response to this feedback. In addition, changes to the catchment delineations, land use classifications, land application rates, and irrigation sources and allocations made during the CV-SALTS and Westside Salt Assessment Project impacted the quality of the model simulations. The calibration was then modified again where possible to correct and account for those changes and to improve the simulations.

Hydrologic Calibration

Hydrologic calibration is the process of adjusting the coefficients of the rainfall-runoff model within WARMF so that the simulations of streamflow match the observations as well as possible. There are three levels of hydrologic calibration: global, seasonal, and event. Global calibration is the process of matching the simulated annual volume of water passing a gage to the volume measured at the gage. In seasonal calibration, the simulated seasonal variation of streamflow is compared and adjusted to follow the same pattern on a measured hydrograph (i.e., a graph of streamflow rising and falling over time). The measured hydrograph typically has a period of high flow during the rainfall season and a recession to base flow during the dry season. Event calibration is the process of matching the simulated peak flows to the observed peaks during precipitation events.

Some representative hydrologic calibration results are shown in Figure 2.1 through Figure 2.3 below. Simulation results are shown in blue lines and observed data in black circles. Ideally, the blue lines pass through all the black circles. Differences in the simulations and observations occur because of a combination of model error (e.g. due to model approximations of complex natural processes), data and input error (e.g. incorrect assumptions about irrigation application, drainage patterns, or return flows), and data measurement uncertainty (e.g. error in measured precipitation or streamflow data). During the calibration process, coefficients were adjusted so that large systematic differences were removed and an overall balance was achieved between positive and negative errors (i.e. simulations were not consistently too high or too low indicating that differences are due primarily to random errors in data rather than coefficient values).

The flow calibration for water years 2000-2007 is shown below for three gaging stations along the San Joaquin River (Lander Avenue (Stevinson), Crows Landing, and Vernalis). Lander Avenue is the upstream boundary condition on the river. Crows Landing is between the confluences of the Merced and Tuolumne Rivers. Vernalis is downstream of all the major east side tributaries. Calibration statistics are listed in Table 2.1. Visual inspection of Figures 2-1 through 2-3 and the values of the calibration statistics (e.g. low relative error and high correlation) demonstrate that the match between simulated and observed flow is good for all three calibration points. Since Lander Ave. is one river segment below the upstream boundary condition, which uses observed data as inflow, the simulation at that location is nearly identical to the observed.

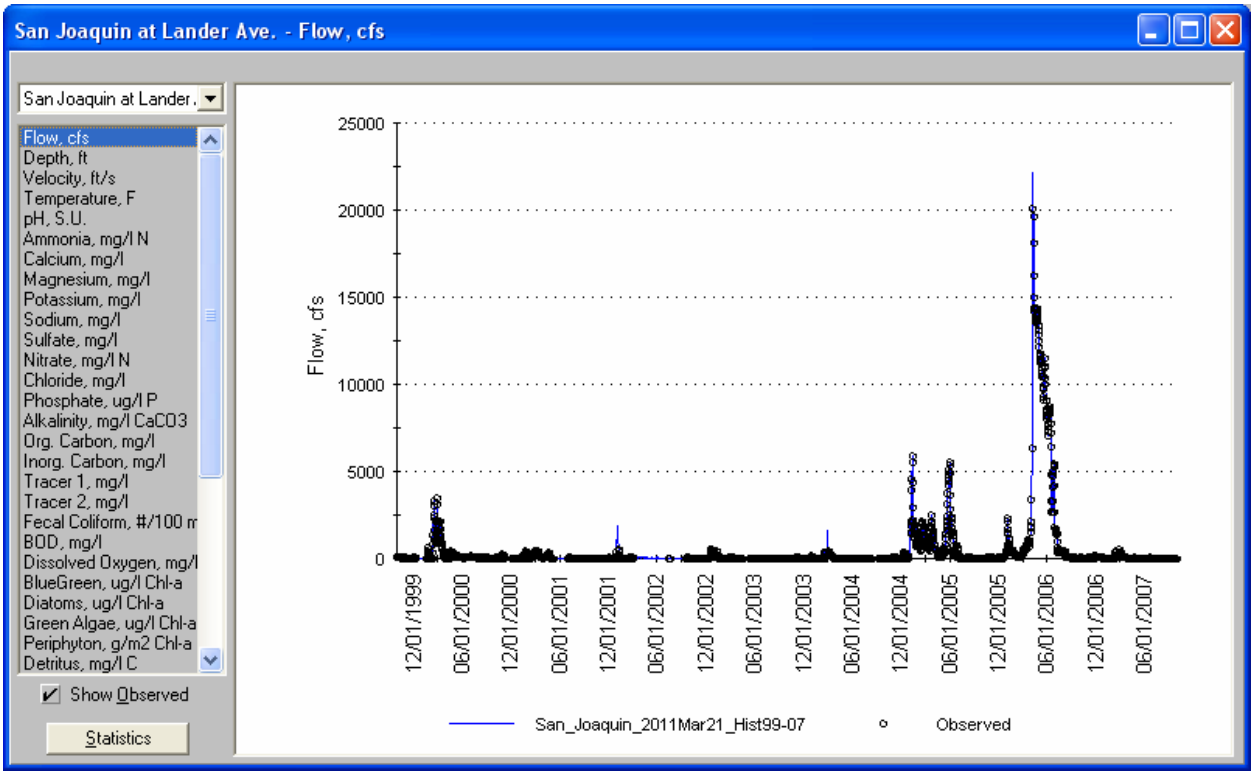

Figure 2.1 Simulated vs Observed Flow at San Joaquin River at Lander Ave. (Stevinson)

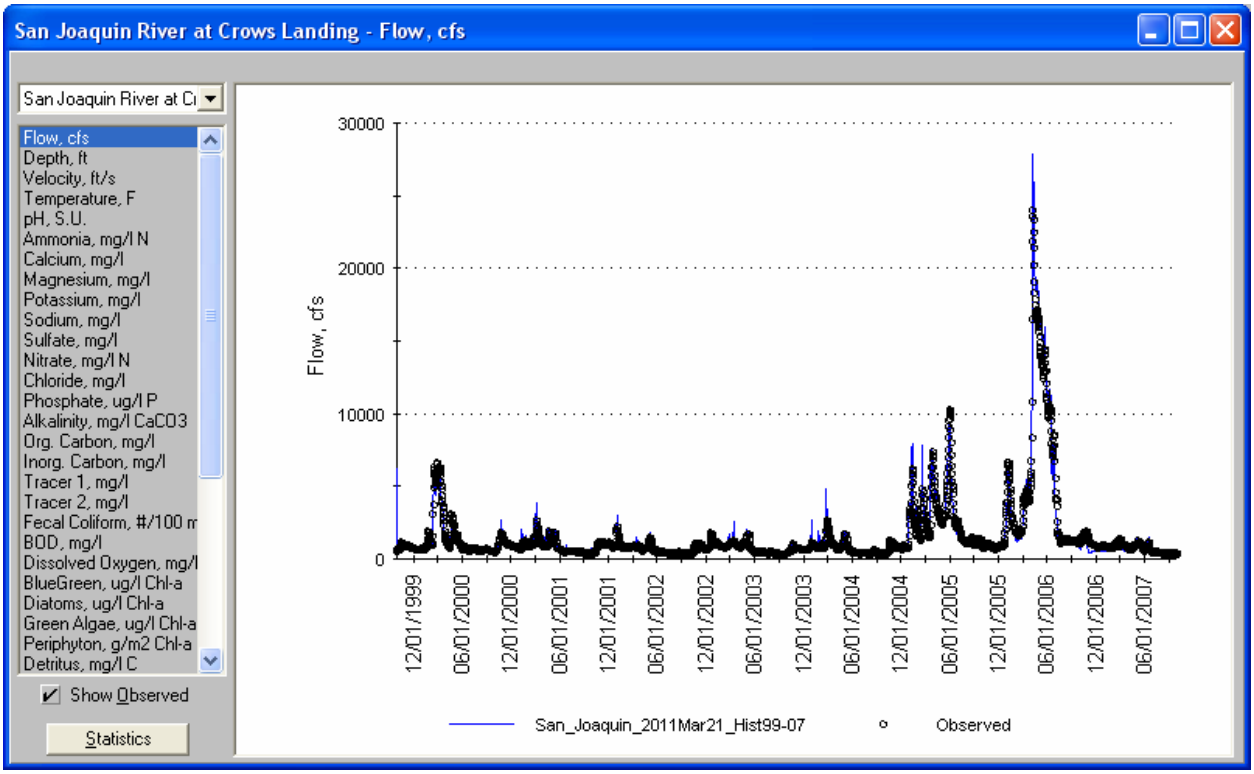

Figure 2.2 Simulated vs Observed Flow at San Joaquin River at Crows Landing

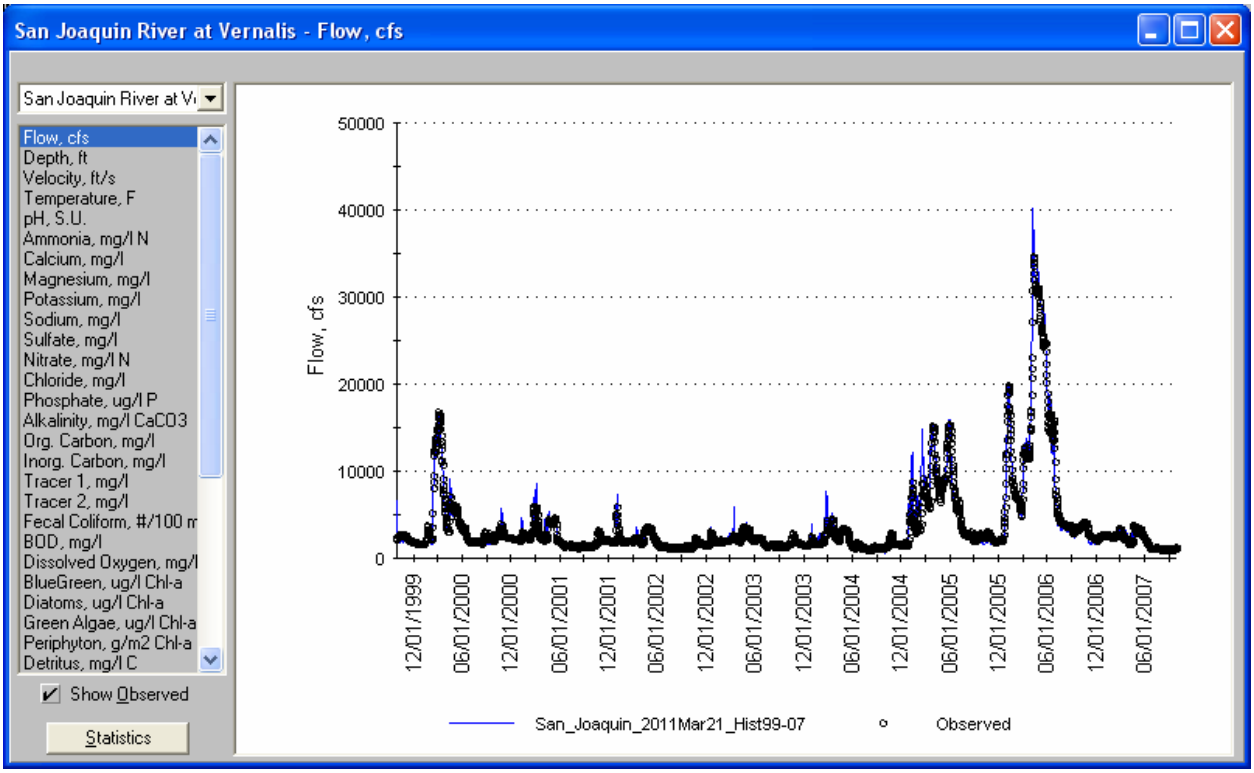

Figure 2.3 Simulated vs Observed Flow at San Joaquin River at Vernalis

Table 2.1 San Joaquin River Flow Calibration Statistics

Gaging Station	% Relative Error	% Absolute Error
San Joaquin River at Lander Ave.	+0.06%	0.68%
San Joaquin River at Crows Landing	+2.1%	18.4%
San Joaquin River at Vernalis	+0.63%	14.1%

Water Quality Calibration

The water quality parameters simulated by WARMF are interdependent. Flow affects the relative percentages of various sources which are mixed together. The travel time is the limiting factor for phytoplankton growth. Temperature is affected by river depth and light penetration but in turn affects reaction rates. Suspended sediment adsorbs some constituents (including nutrients, organic carbon and some components of TDS) which can then be sequestered or released as the sediment settles to the river bed or is scoured during high flow. Nutrients, temperature, and light all affect phytoplankton growth, which converts inorganic carbon into organic carbon.

The San Joaquin River DO TMDL Upstream Studies Task 6 Report (Herr, Chen, and van Werkhoven 2008) and the Salt and Nitrate Pilot Implementation Study Report (Larry Walker & Associates et al, 2010) include detailed discussions of the calibration of water quality parameters which in turn affect nutrients, TDS and organic carbon, the constituents of primary concern to the Drinking Water Policy Work Group. The discussion here focuses on the calibration of the various forms of nutrients, TDS and organic carbon. These constituents differ greatly in how they interact with other parameters simulated by WARMF. For example, organic carbon comes from a combination of decayed plant matter, phytoplankton, and point sources.

The calibration is shown for three water quality stations along the San Joaquin River: Lander Avenue (Stevinson), Crows Landing, and Vernalis. Lander Avenue is the upstream boundary condition on the river. Crows Landing is between the confluences of the Merced and Tuolumne Rivers. Vernalis is downstream of all the major east side tributaries.

The following sections describe the calibration results for nutrients (NH4, NO3, and PO4), TDS (using two EC measures) and organic carbon (dissolved and total). For each water quality parameter, the simulated results (blue lines) and observed data (black circles) are compared from the most upstream station to the most downstream station.

Total Dissolved Solids / Electrical Conductivity

Since TDS is largely conservative, calibration is a matter of accounting for the correct amount of salt at upstream boundary conditions and in the nonpoint source load to shallow groundwater. Because it is easily measured, there is generally ample data to characterize the upstream boundary conditions. The load from shallow groundwater is largely a function of mass balance. Irrigation water from various sources is applied to the land using the water quality of the water source. Thus, water diverted from the San Joaquin River introduces more salt to the shallow groundwater than water from the Delta-Mendota Canal or the Tuolumne River. Assumptions regarding the relative amount of the various irrigation sources applied to a catchment can have a significant impact on the quality of TDS/EC simulations.

WARMF simulates the evapotranspiration of water from the soil and the resulting concentration of dissolved ions within the remaining groundwater. The model simulates the subsurface flow

including the dissolved ions and exfiltration to the San Joaquin River and its tributaries within the model domain.

There are two parameters used in calibration to adjust the amount of evapotranspiration: magnitude adjustment and skewness (seasonal) adjustment. These parameters are described in the WARMF Technical Documentation (Chen, Herr, and Weintraub 2001). Although these parameters have an important effect on concentration of TDS in shallow groundwater, they were only adjusted to calibrate the simulation of flow. The initial soil pore water concentrations of the various ions (NH_4, Ca, Mg, K, Na, SO_4, NO_3, Cl, PO_4, inorganic carbon) can impact simulation results because the soil stores a large quantity of ions. Rather than calibrate these initial concentrations, it was assumed that there would be minimal long-term trend in ionic concentrations in the soil. Thus, the initial concentrations were set approximately equal to the concentration at the end of the simulation in each soil layer of each catchment. The TDS/EC calibration is presented using the "Calculated EC" parameter, which is calculated within WARMF as the sum of the individual ions of which it is composed.

Calculated EC

Figure 2.4 through Figure 2.6 compare the predicted and observed time series of calculated EC at various stations along the San Joaquin River. Calculated EC takes into account processes which can affect ions as they are transported throughout the watershed, including adsorption, settling, and equilibration of inorganic carbon with the atmosphere.

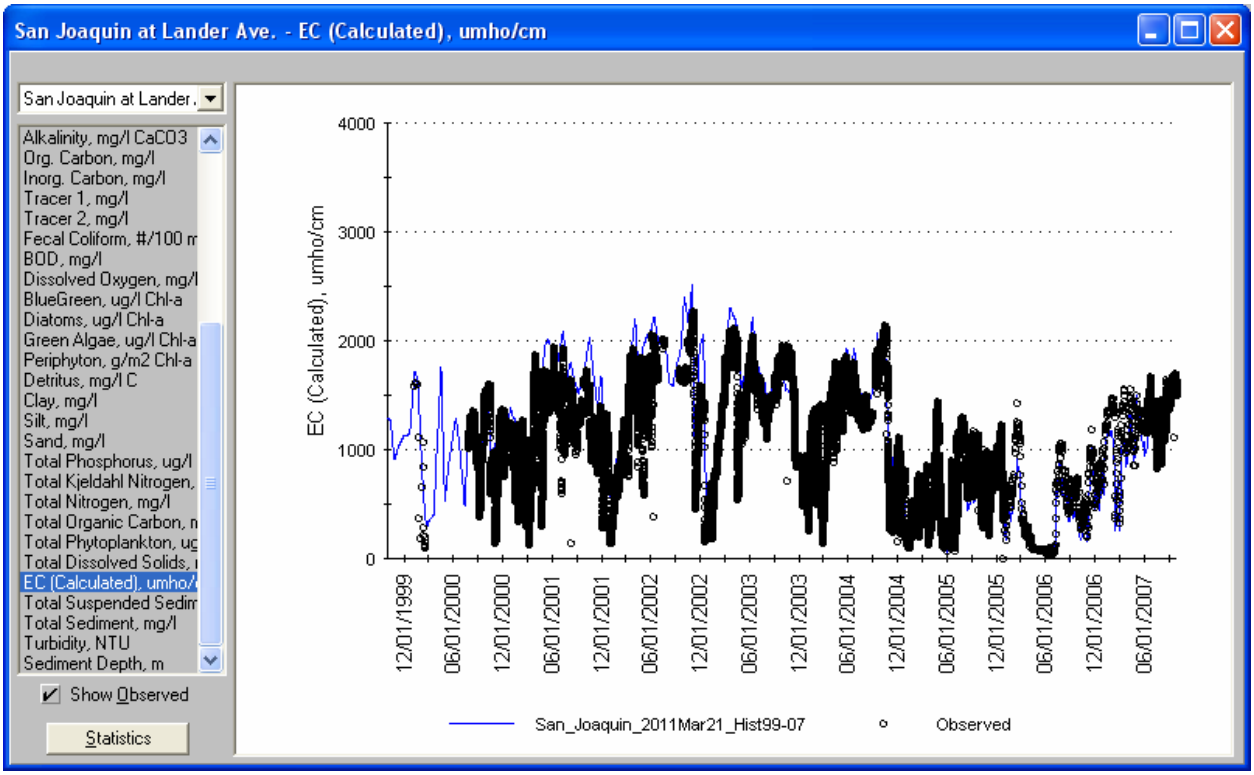

Figure 2.4 Simulated vs Observed EC at Lander Ave. (Stevinson)

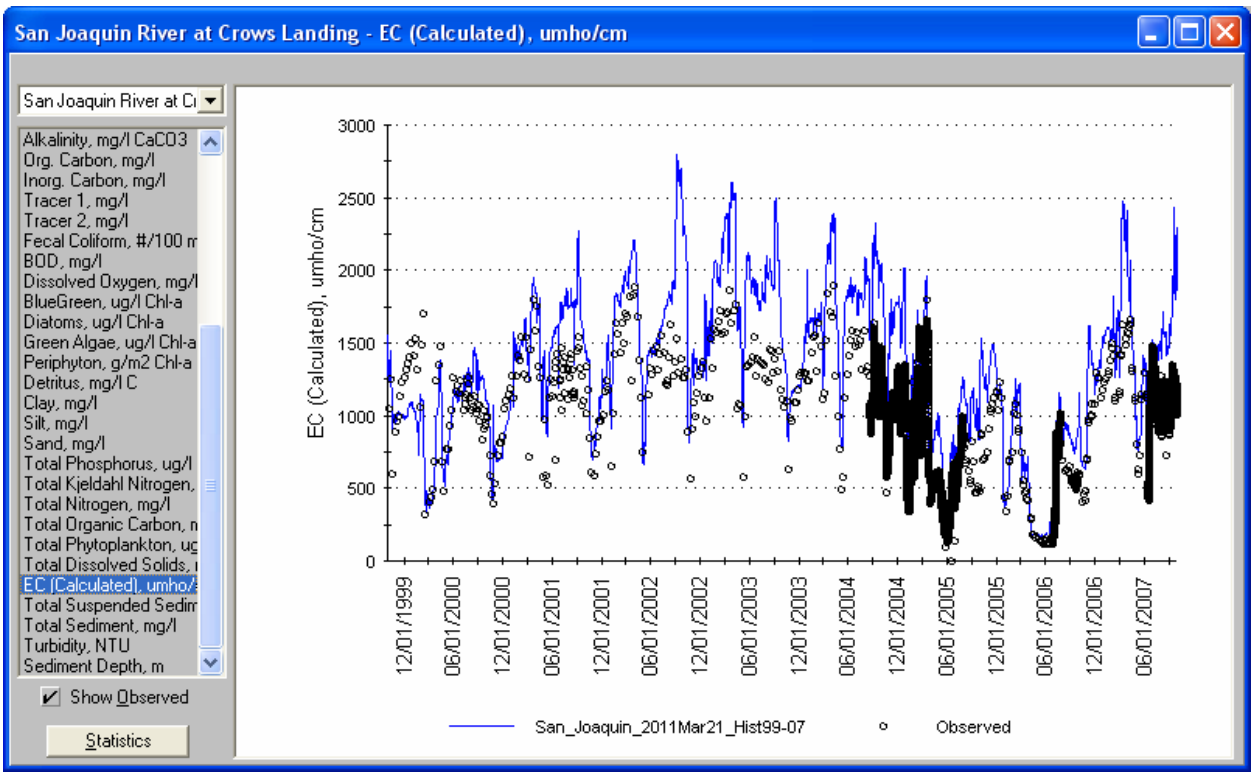

Figure 2.5 Simulated vs Observed EC at Crows Landing

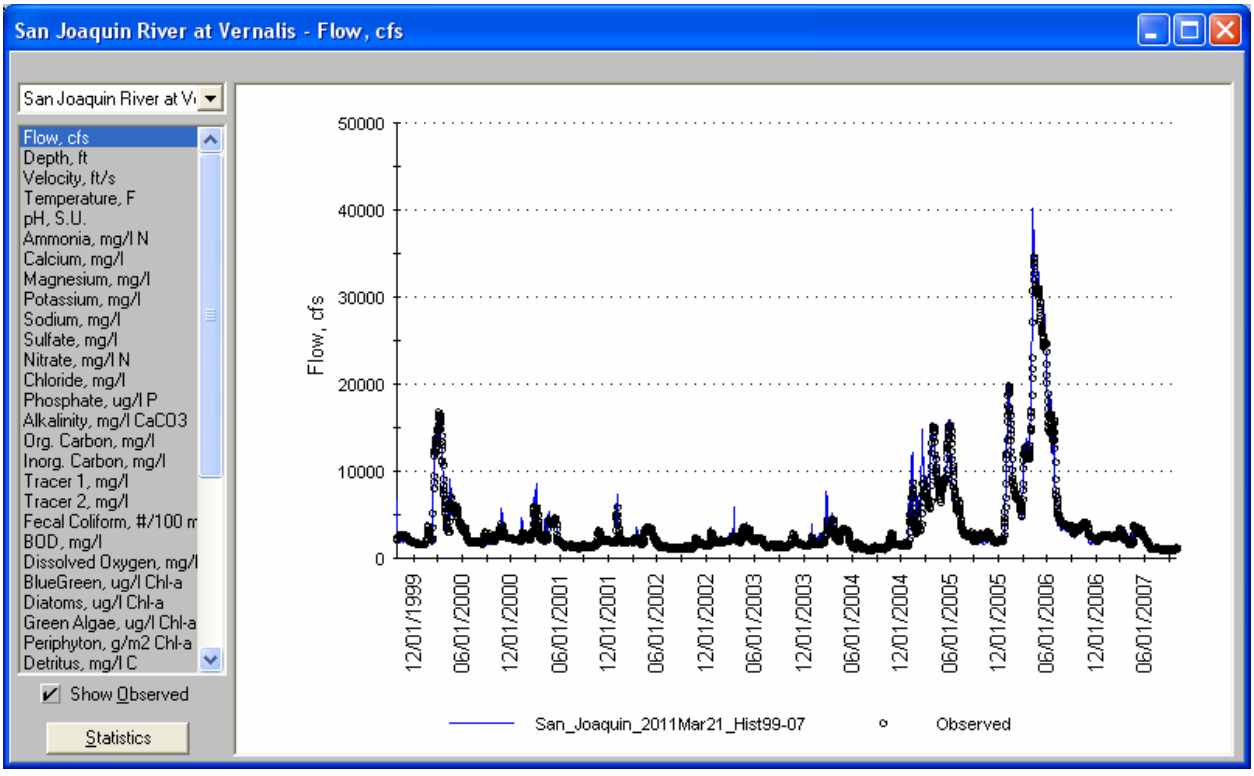

Figure 2.6 Simulated vs Observed EC at Vernalis

Table 2.3 shows the model errors for calculated EC at the monitoring stations on the San Joaquin River. The errors are low at the Lander Avenue monitoring station, indicating that little model bias is introduced in the short reach below the boundary condition. The errors are higher at Crows Landing and Vernalis, reflecting a large positive bias introduced to the model between Lander Avenue and Crows Landing. Further investigation of model output revealed that the bias originated primarily in the Salt and Mud Slough subcatchments, which join the San Joaquin River between the Lander Avenue and Crows Landing monitoring stations. Since TDS and EC are largely conservative measurements, as explained previously, simulations of TDS/EC are controlled mainly by the upstream or non-point source loads entering the river and shallow groundwater. Thus errors in these simulations are usually due to incorrect assumptions regarding such input loads. Irrigation practices, fertilizer application, and drainage patterns in particular are not well known and documented throughout the Westside region of the San Joaquin Valley. Many assumptions were necessary in order to estimate the amounts of irrigation water applied to each catchment and from which sources the water originated. To improve the calibration of EC in the San Joaquin River, these assumptions would need to be revisited and revised.

Table 2.2 Model Errors in EC in the San Joaquin River

Monitoring Station	Relative Error	Absolute Error
Lander Avenue (Stevinson)	+6.8%	18%
Crows Landing	+25%	26%
Vernalis	+21%	25%

Organic Carbon

In WARMF, organic carbon includes a combination of compounds from a variety of sources. It includes the humic and fulvic acids resulting from the decay of leaf litter on land and also living and dead phytoplankton. It can also come from point source discharges, urban runoff, and animals. Like total dissolved solids, organic carbon is also recycled from the San Joaquin River through agricultural fields and back to the river as nonpoint source load.

Dissolved Organic Carbon

Figure 2.7 through Figure 2.9 compare the time series of simulated and observed dissolved organic carbon at various stations along the San Joaquin River. The match for predicted and observed dissolved organic carbon concentration was generally good for all stations, but the model did not predict some measured peak concentrations at Vernalis. Refer to the total organic carbon calibration section for discussion regarding winter peak concentrations.

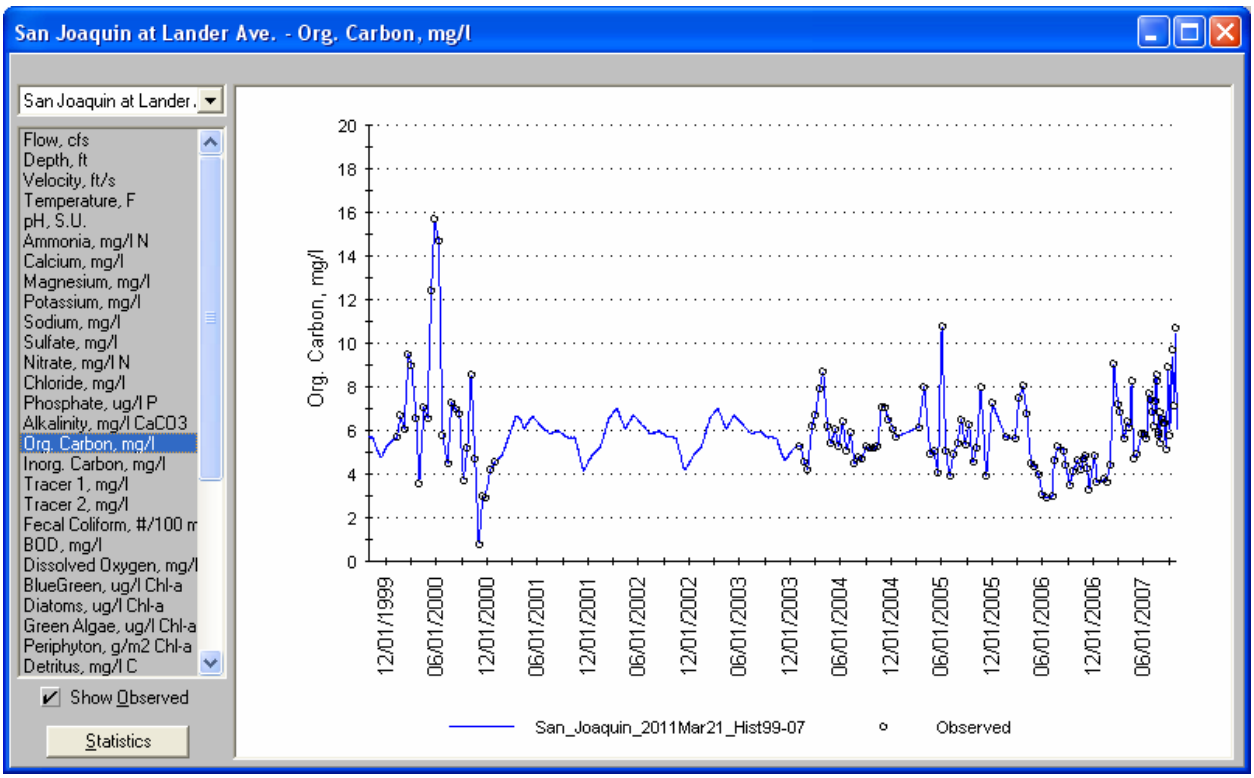

Figure 2.7 Simulated vs Observed Dissolved Organic Carbon at Lander Avenue

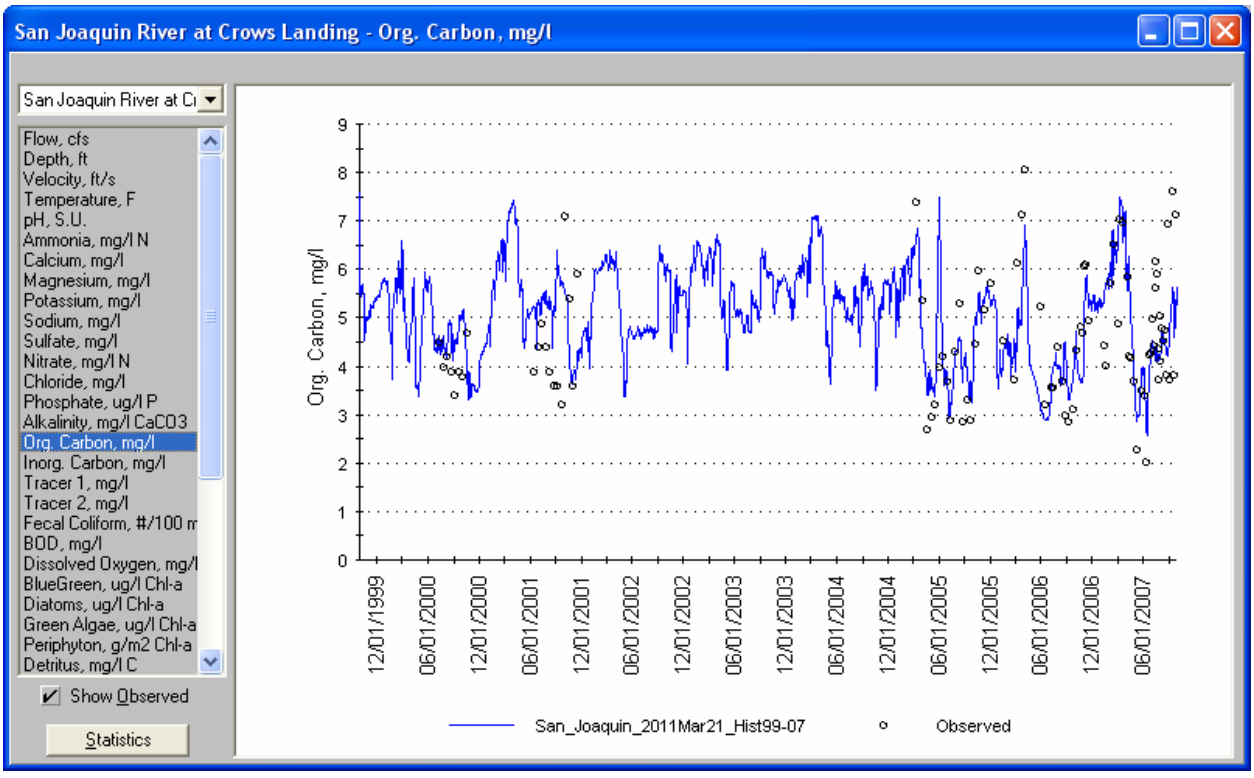

Figure 2.8 Simulated vs Observed Dissolved Organic Carbon at Crows Landing

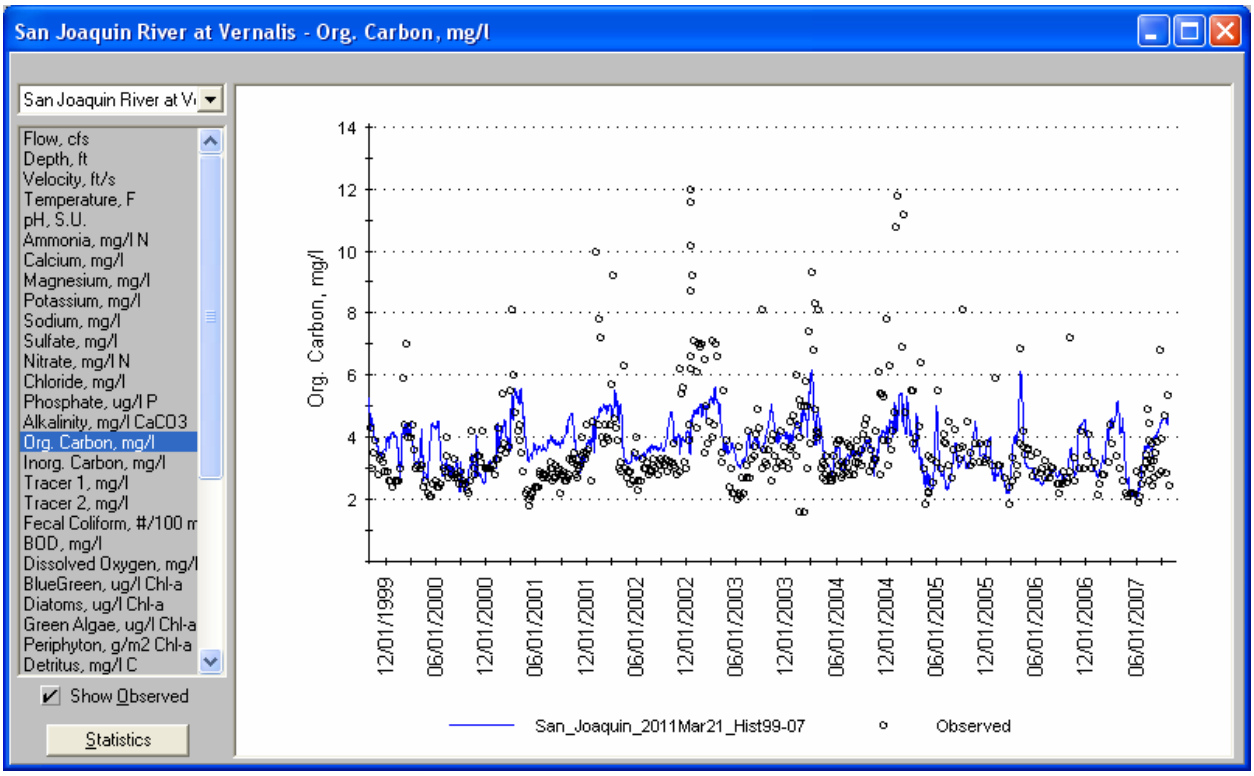

Figure 2.9 Simulated vs Observed Dissolved Organic Carbon at Vernalis

Table 2.3 shows the model errors of dissolved organic carbon at various monitoring stations on the San Joaquin River. Monitoring for organic carbon was done most frequently at Vernalis. Although the relative error is very low there, Figure 2.9 shows the underprediction of winter peak concentrations in 2000-2005. The possible causes of this error are discussed later in this section. In other seasons, the simulations track the measured data well.

Table 2.3
Model Errors of Dissolved Organic Carbon Concentration in the San Joaquin River

Monitoring Station	Relative Error	Absolute Error
Lander Avenue (Stevinson)	-0.3%	0.8%
Crows Landing	+1.6%	16.4%
Vernalis	+1.8%	24%

Total Organic Carbon

Figure 2.10 through Figure 2.12 compare the time series of predicted and observed total organic carbon concentration. Total organic carbon includes dissolved organic carbon, organic carbon adsorbed to suspended sediment, and biological organic carbon in phytoplankton and detritus.

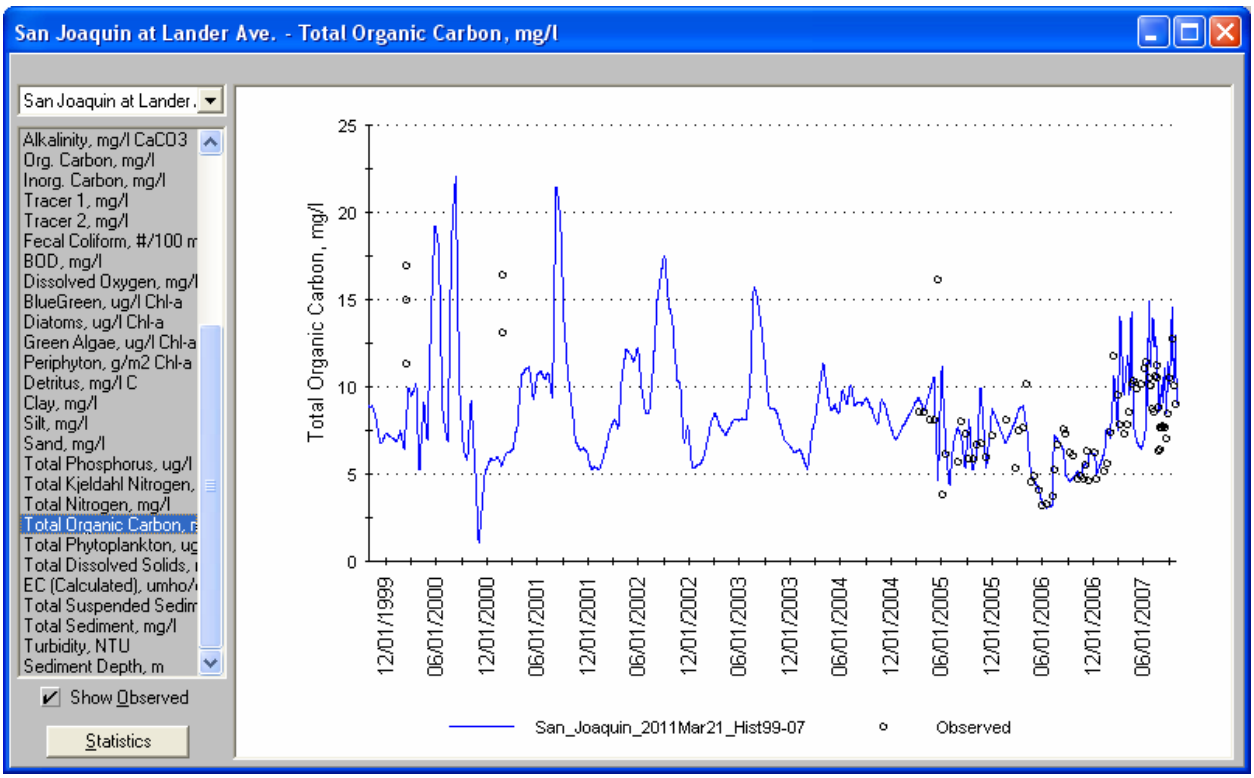

Figure 2.10 Simulated vs Observed Total Organic Carbon at Lander Avenue

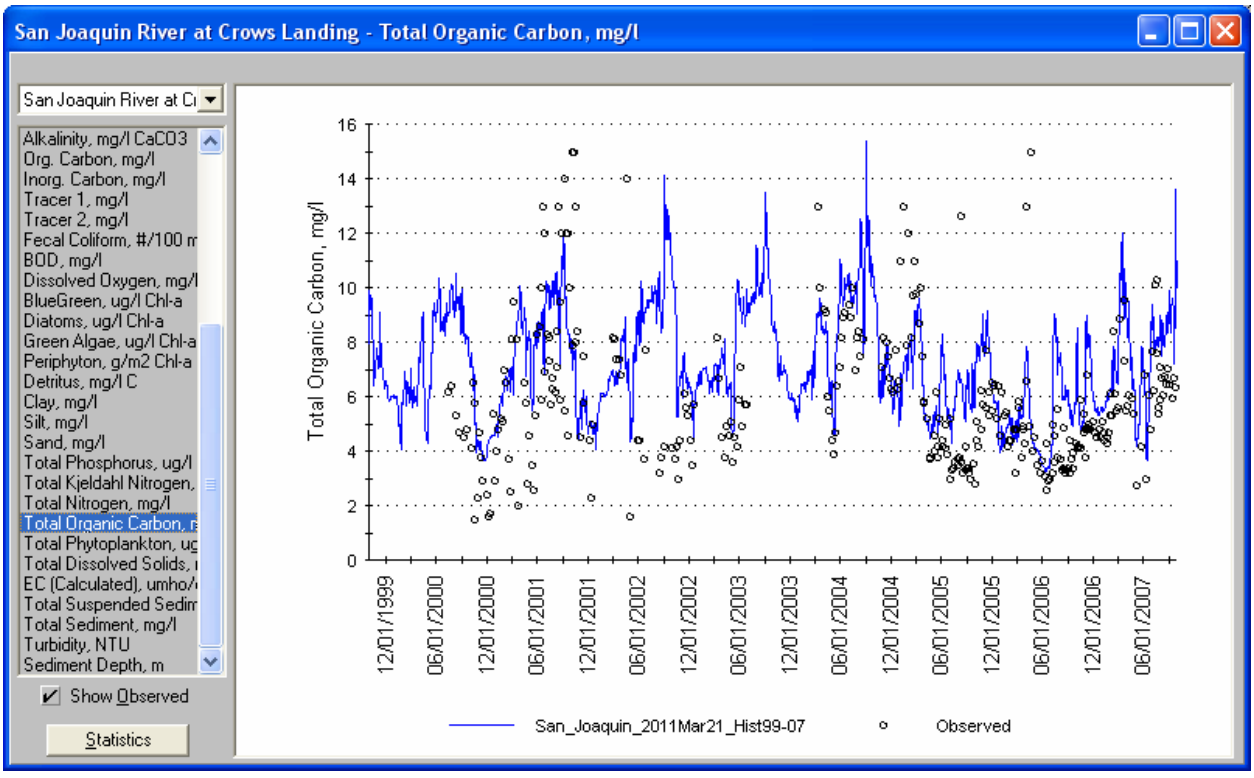

Figure 2.11 Simulated vs Observed Total Organic Carbon at Crows Landing

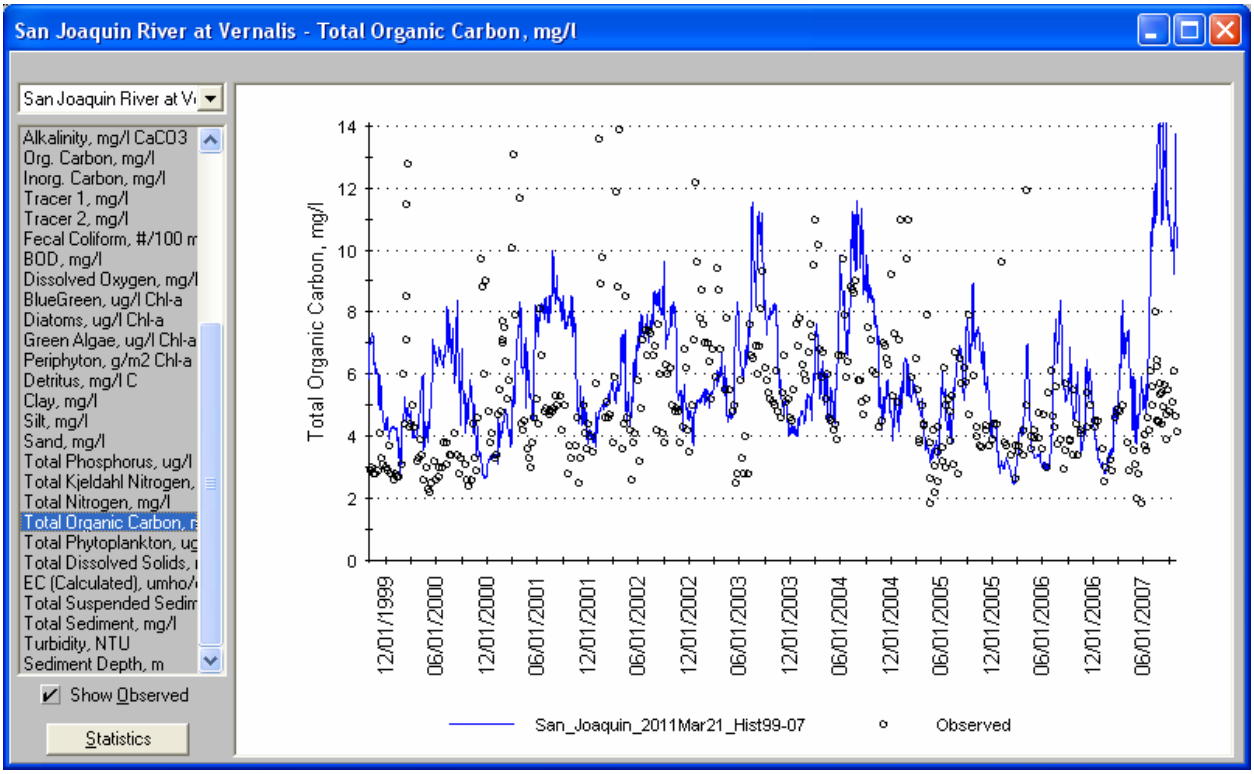

Figure 2.12 Simulated vs Observed Total Organic Carbon at Vernalis

Table 2.4 shows the model errors for total organic carbon at various monitoring stations on the San Joaquin River. As with dissolved organic carbon, more total organic carbon monitoring data was collected at Vernalis than at other stations. There are two reasons why the absolute error is greater than 30%, the goal of calibration, at Vernalis. As with dissolved organic carbon, the simulation does not capture peak winter concentration of organic carbon. Unlike dissolved organic carbon, simulated total organic carbon was significantly higher than measured in the summers of 2000-2002. The possible causes of these errors are described in the following section of this report.

Table 2.4
Model Errors for Total Organic Carbon in the San Joaquin River

Monitoring Station	Relative Error	Absolute Error
Lander Avenue (Stevinson)	3.7%	24.8%
Crows Landing	16.1%	28.4%
Vernalis	11.4%	38.0%

Errors in Organic Carbon Simulation

In revisiting the calibration of WARMF for the San Joaquin River, the causes of the summer and winter errors in simulations of organic carbon were investigated. Each could be a case of model error, data error, a combination of the two. The data was primarily collected by the California Department of Water Resources, a data source which does not raise concerns about data quality.

Winter Organic Carbon Concentration Peaks

For the failure of the model to predict the winter peak concentrations of both dissolved and total organic carbon, there are multiple possibilities:

- Storm runoff from urban areas is causing the measured concentration peaks but are not being simulated correctly
- Storm runoff from confined feeding operations or other agricultural lands is causing the measured concentration peak but are not being simulated correctly
- Winter organic carbon concentration is not represented correctly in tributary inflows

To determine the correlation between local precipitation and total organic carbon concentration at Vernalis, we can plot them together. Figure 2.13 and Figure 2.14 show measured total organic carbon at Vernalis and precipitation measured at Modesto for February-March of 2000 and 2001, respectively. In 2000, the total organic concentration peak comes 1-3 days after a 3 cm precipitation event. This implies a source of organic carbon related to storm flow.

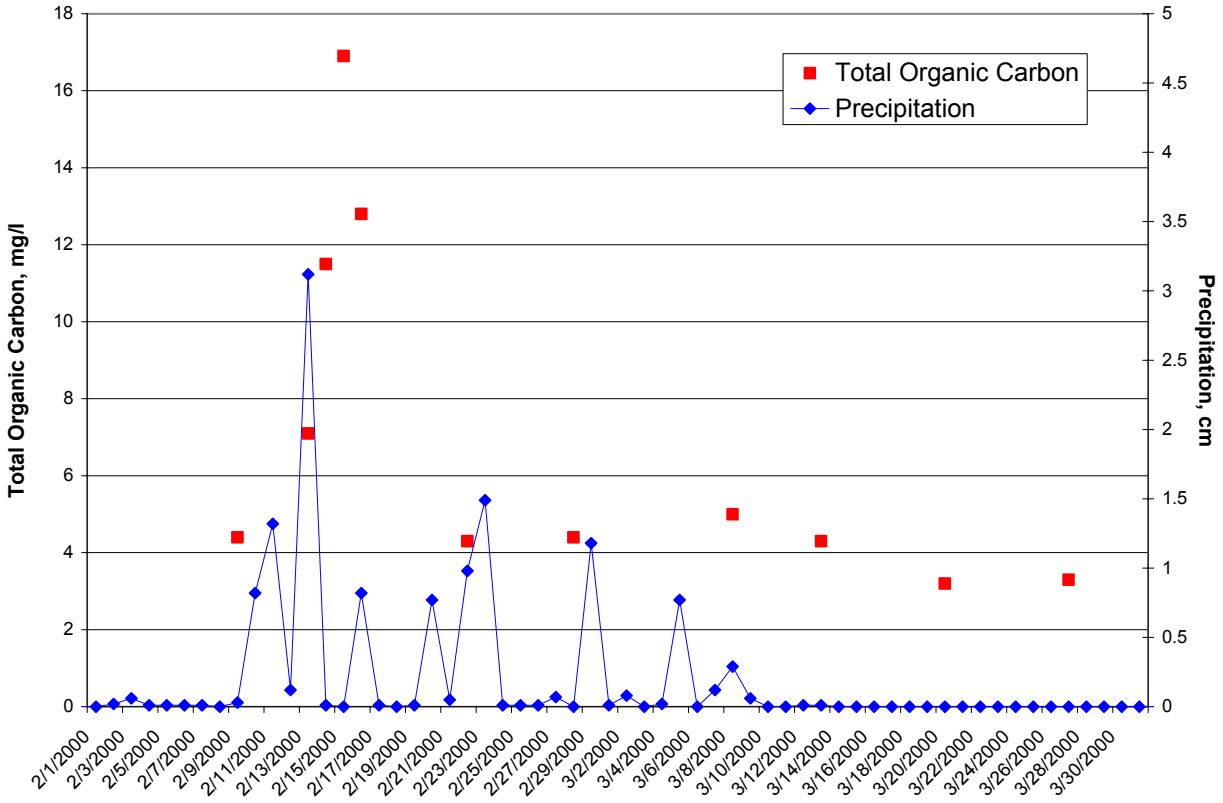

Figure 2.13 Measured Total Organic Carbon and Precipitation, February-March 2000

In Figure 2.14 showing February-March 2001, the total organic carbon concentration is elevated before, immediately after, and also weeks after a 2.6 cm rainfall event. Unlike the year 2000, storm runoff does not appear to be a good explanation for the measured peak organic carbon concentration in February and March.

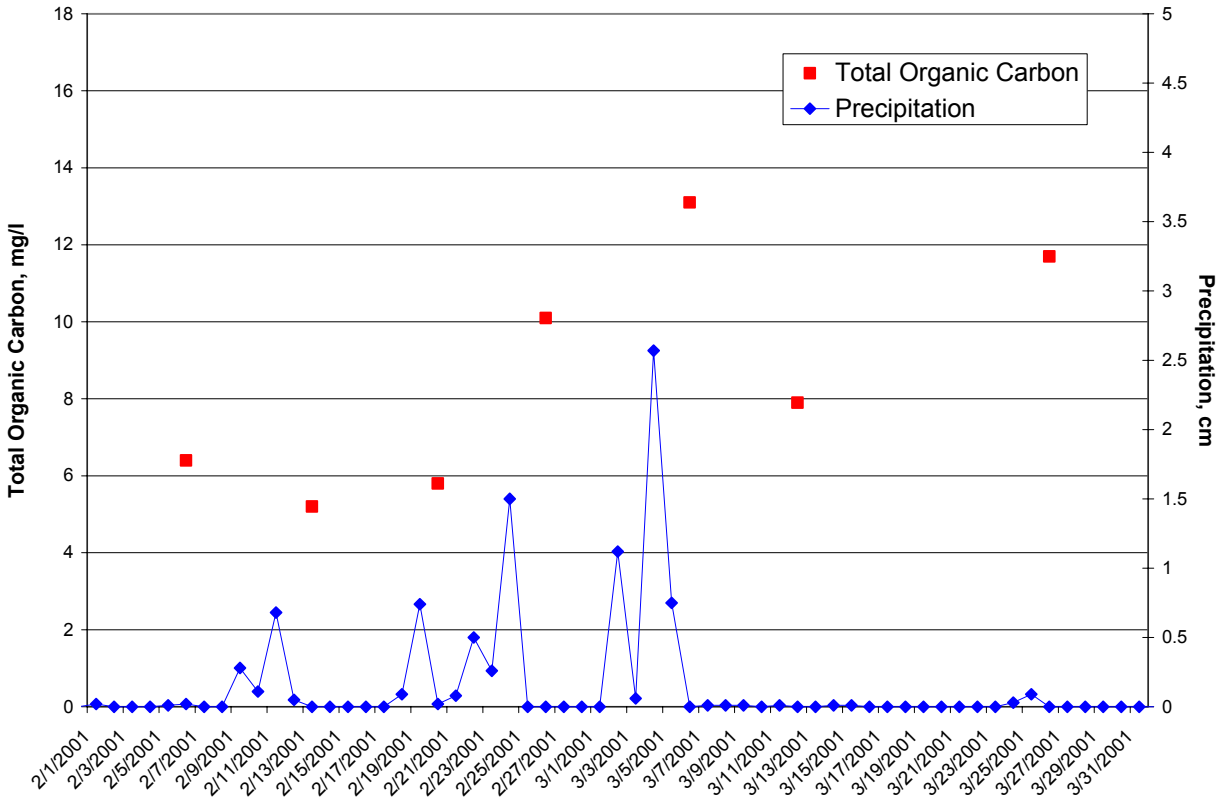

Figure 2.14 Measured Total Organic Carbon and Precipitation, February-March 2001

To test the local storm runoff hypothesis, a WARMF simulation was run with a very large land application rates to determine if winter storms could be causing significant runoff of organic carbon. The model's original application rates of organic carbon were multiplied by 100 for residential and commercial land uses. The new loading rates were set to 50 and 100 kg/ha/month respectively in each land use for the test simulation. With unrealistically high application rates, a response in the model should be apparent. Figure 2.15 shows the result of the test in green with the base case simulation in blue. Although the test case shows concentration spikes of up to 2 mg/l from the unrealistically high urban land application rates, the observed concentration spikes are closer to 10 mg/l. Urban runoff from land within the WARMF model domain is thus not an explanation for the discrepancy between simulated and measured organic carbon.

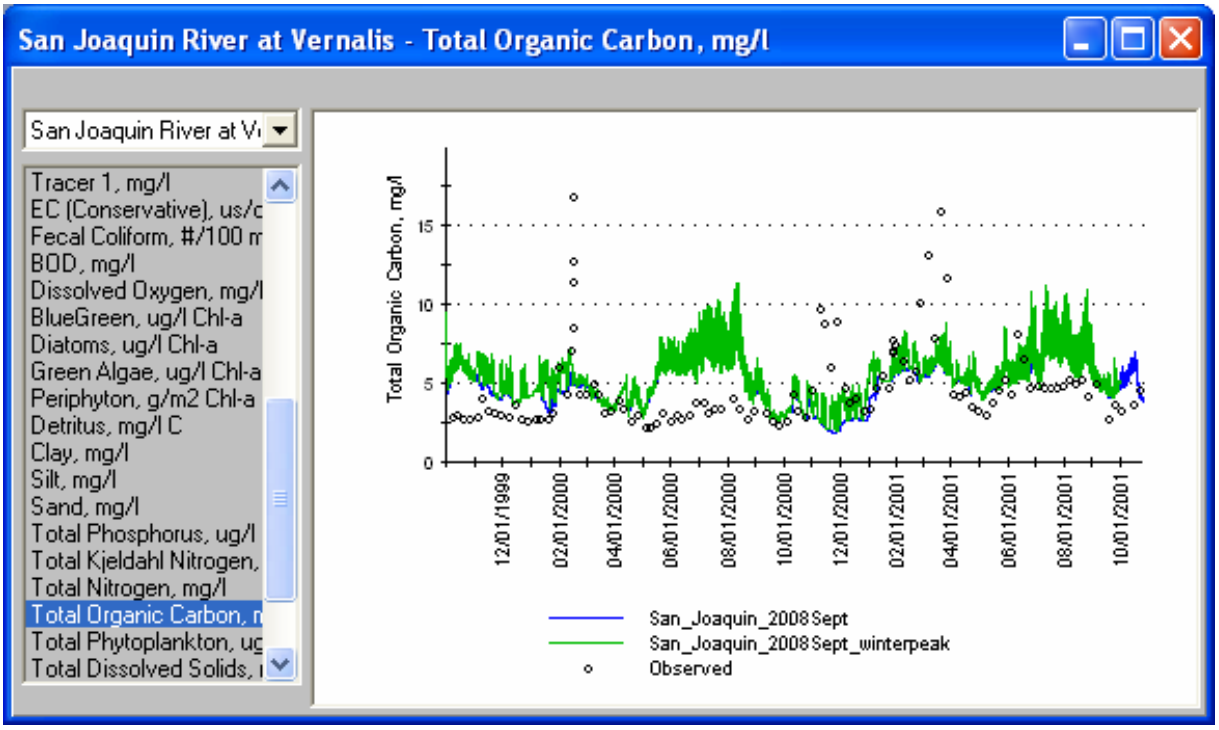

Figure 2.15 Test of 100X Organic Carbon Loading from Urbanized Land Uses

The organic carbon concentration peak of February 13-16 of 2000 coincides with rapidly increasing flow of the San Joaquin River at Vernalis as shown in Figure 2.16. The origin of that flow increase was the Merced and Tuolumne Rivers. Although the source of the organic carbon could have been within reservoir releases, the increasing flow could also have flushed organic matter from the riparian zone of the rivers which had previously been above the water level. The similar time period from 2001, shown in Figure 2.17 does not show such a clear relationship between rising flow and high organic carbon concentration. The organic carbon concentration persists at over 10 mg/l after the flow peak has risen and receded.

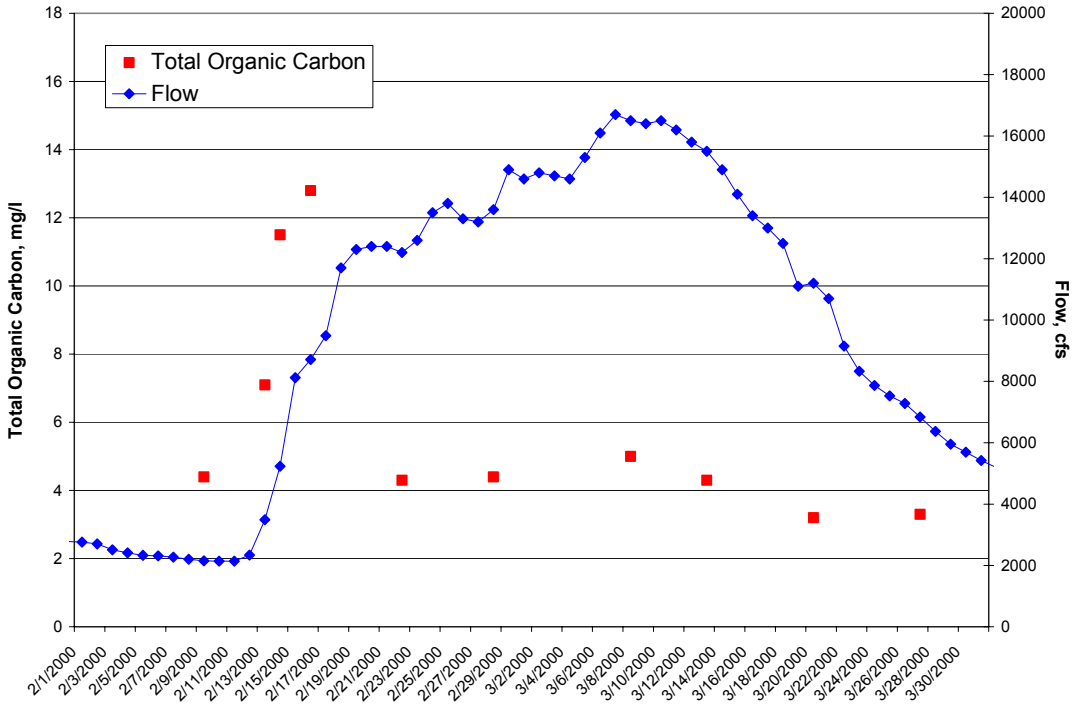

Figure 2.16 Measured Total Organic Carbon and Flow at Vernalis, February-March 2000

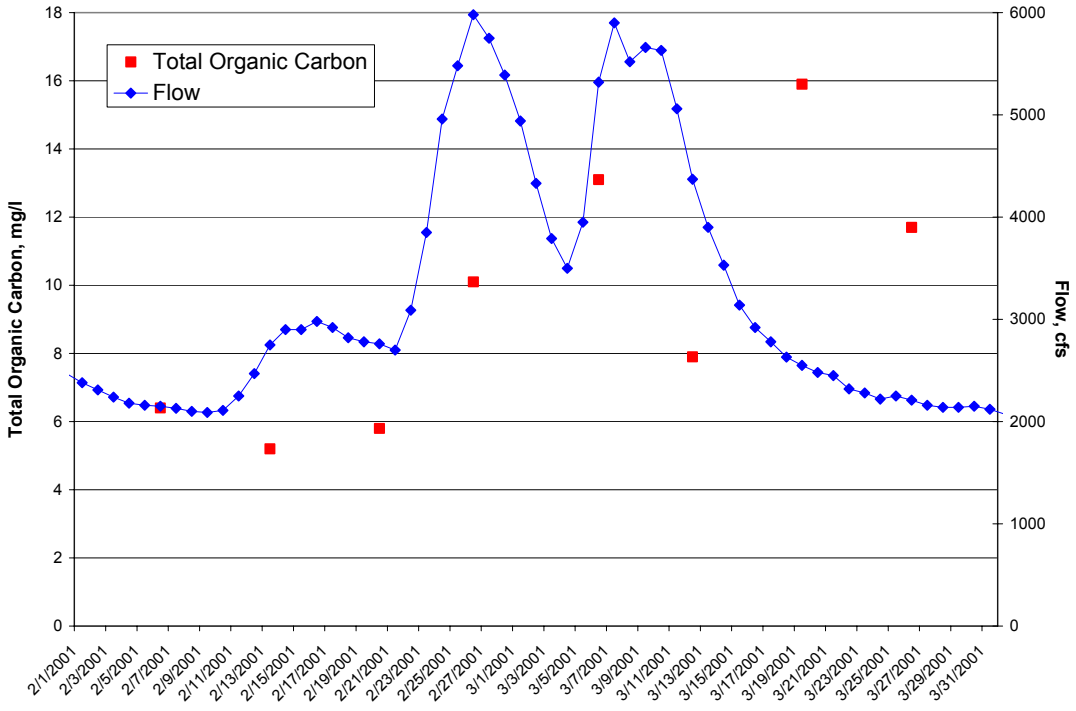

Figure 2.17 Measured Total Organic Carbon and Flow at Vernalis, February-March 2001

Another potential source of error between model predictions and measured data is insufficient data at the upstream boundary conditions. The peak concentration events could be occurring

outside the model domain in one or more tributaries to the San Joaquin River. There was no organic carbon data for the tributaries in 2001, so the inflows were assumed to have average concentrations for that time of year based on other years for which there was data. Although organic carbon data was collected for the tributaries in 2000, no data happened to be collected in the tributaries from February 13-16 when the concentration peak was observed at Vernalis. The inflow concentrations were interpolated between days when data was collected on either side of the peak time period.

Simulated Summer Organic Carbon Concentration Peaks

The simulated summer peaks of total organic carbon are caused by the carbon in phytoplankton and detritus. For this project, the model was run on a daily time step. When simulating phytoplankton on a daily time step, it has a moderate amount of light 24 hours per day which causes more growth than was actually observed. A test simulation using a 4-hour time step was run to examine the linkages between time step, phytoplankton growth, and total organic carbon. Figure 2.18 and Figure 2.19 show total organic carbon and total phytoplankton, respectively. The daily simulation is shown in blue, the 4-hour time step simulation is in green, and observed data is in black circles. Simulated phytoplankton using a 4-hour time step has much lower concentration than using the daily time step and is a better match to measured data. Using the shorter time step also eliminates the simulated summer peak concentrations of total organic carbon which were not observed in the measured data.

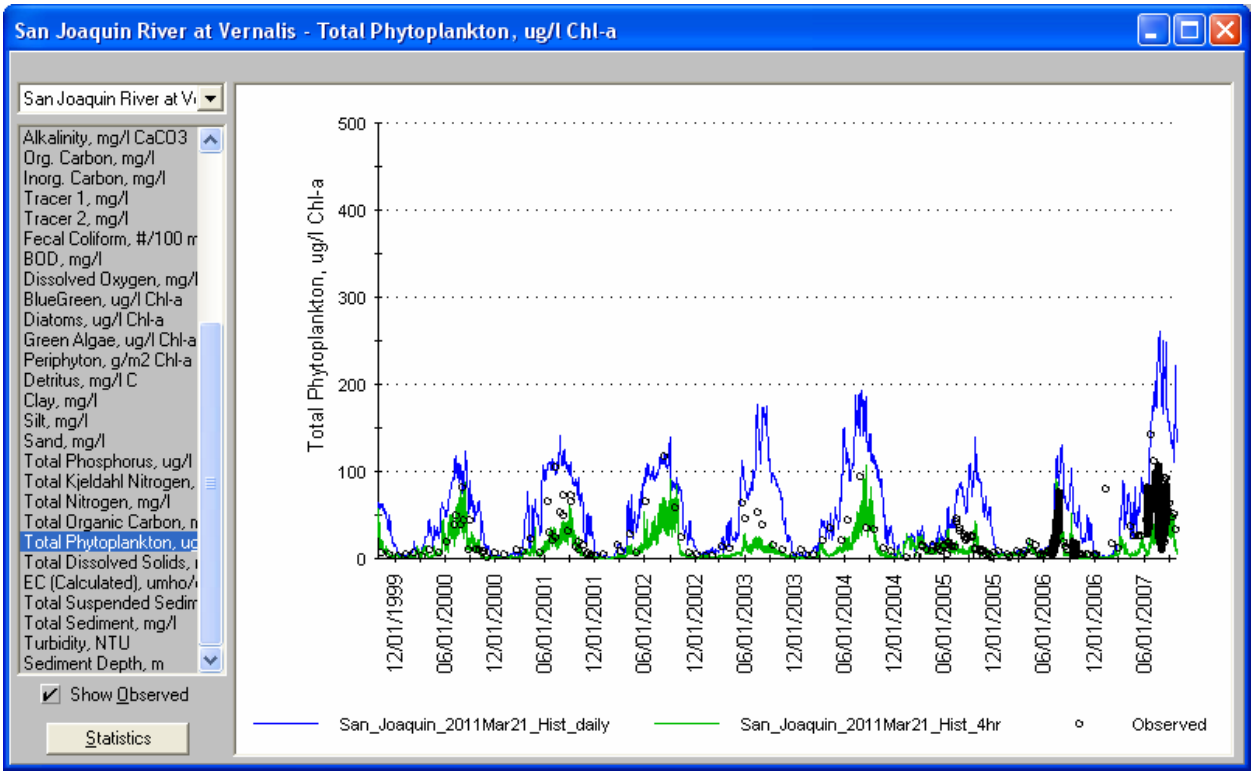

Figure 2.18 Simulated and Observed Phytoplankton, Daily and 4-Hour Time Steps

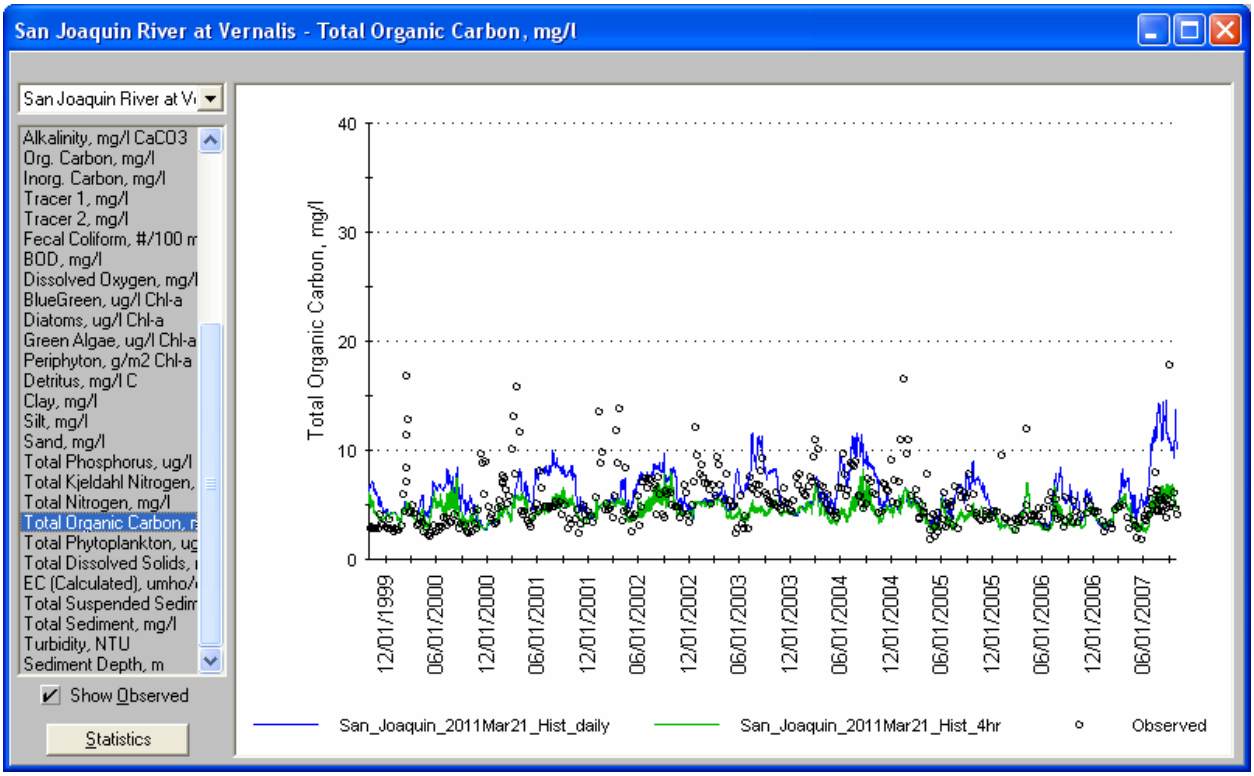

Figure 2.19 Simulated and Observed Total Organic Carbon, Daily and 4-Hour Time Steps

Nutrients

Nutrients simulated in WARMF include ammonia, nitrate, total nitrogen, total Kjeldhal nitrogen, dissolved orthophosphate and total phosphorus WARMF tracks nutrient loadings from their sources, such as atmospheric deposition, point sources, irrigation, and fertilizer application (including animal waste), through the watershed surface and soil layers, accounting for processes of adsorption/desorption and nitrification/denitrification. Calibration results are presented in the following sections for ammonia, nitrate and total phosphorus.

Ammonia

Figure 2.20 through Figure 2.22 compare the time series of predicted and observed ammonia concentration. The match between simulated and observed is good at Lander Ave, near the upstream boundary condition, however it degrades downstream at Crows Landing and Vernalis. Potential sources of error are discussed below.

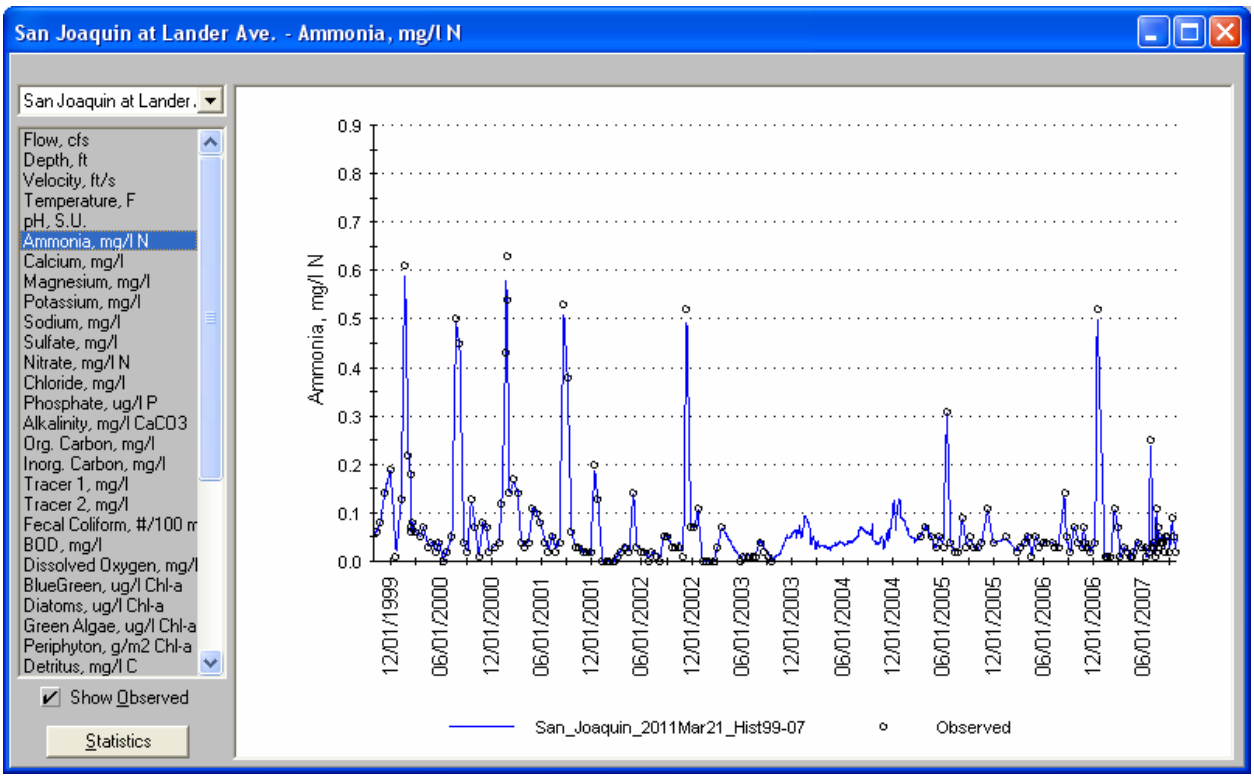

Figure 2.20 Simulated vs Observed Ammonia at Lander Avenue

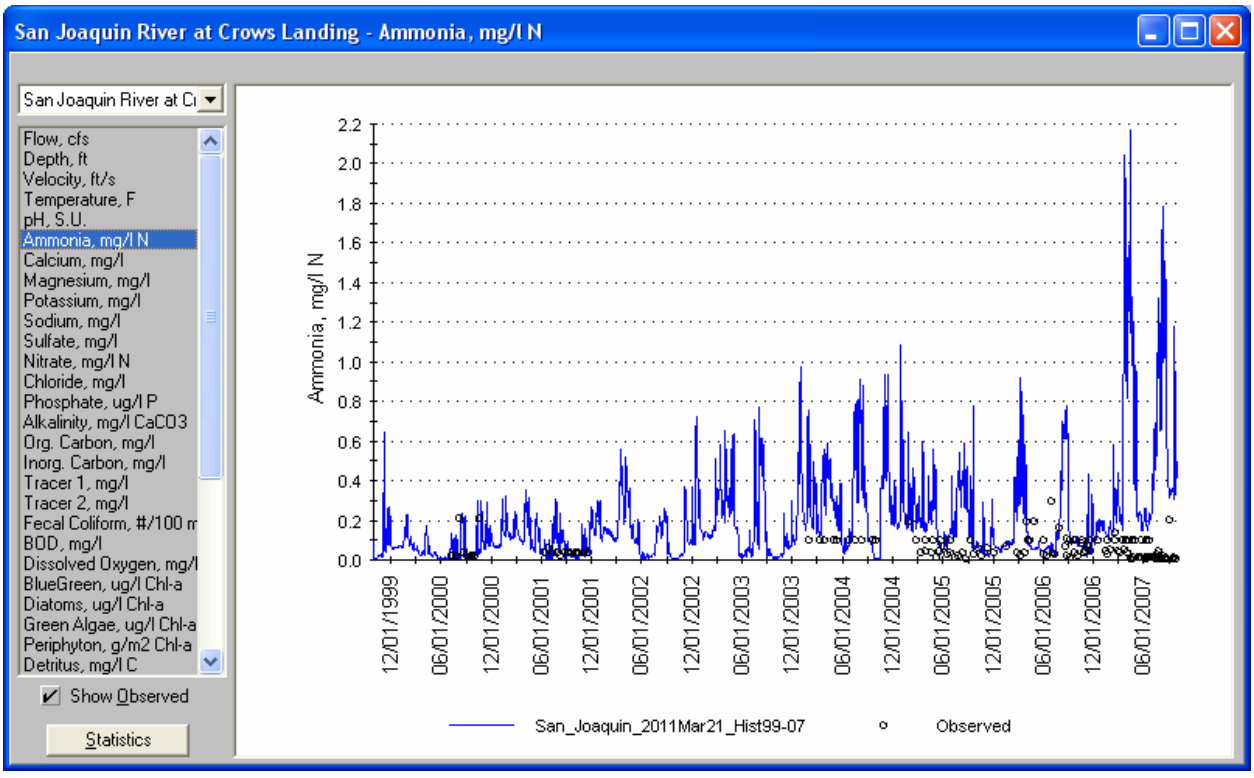

Figure 2.21 Simulated vs Observed Ammonia at Crows Landing

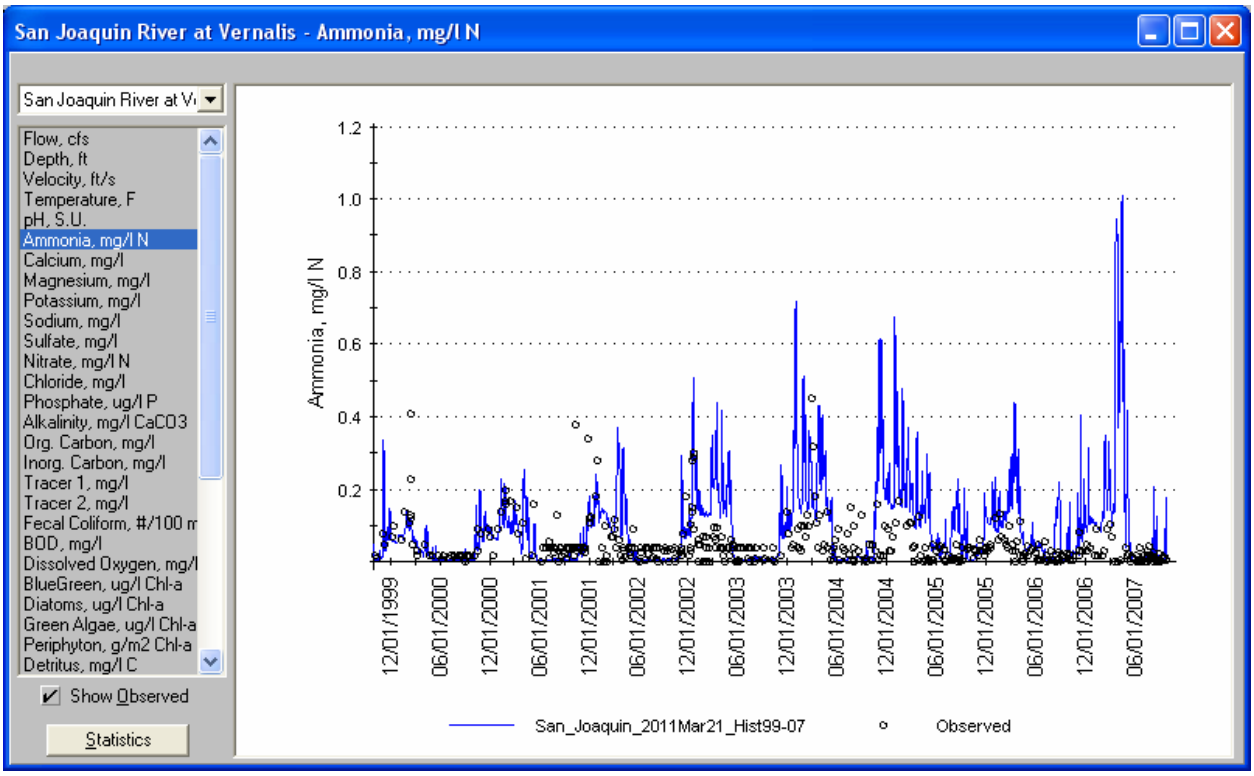

Figure 2.22 Simulated vs Observed Ammonia at Vernalis

Table 2.5 shows the model errors for ammonia at the three presented monitoring locations along the San Joaquin River. The error is low at Lander Avenue, indicating that the upstream boundary inflow is not a major source of error in the ammonia simulation further downstream. The errors are high at both Crows Landing and Vernalis. The main sources of the high ammonia concentrations are dairies, which exist mainly on the east side of the river. Of the total simulated ammonia load to Crows Landing (2810 kg/d), 70% (1984 kg/d) is nonpoint source load coming from dairy land use. Similarly, of the total simulated ammonia load to Vernalis (4944 kg/d), 63% (3146 kg/d) comes from dairy land use. The assumed land application rates of ammonia for dairy land use vary by catchment and are generally very high (see Table 1.4). In dairy-dominated catchments, land application constitutes by far the largest source of ammonia. As one example, in catchment #817, which is 39% dairy land use, land application comprises 93% of the ammonia sources in the catchment. In such cases, adjusting model parameters has very little impact on the resulting ammonia simulation. In order to improve the ammonia calibration downstream of Lander Avenue, the dairy land application assumptions would need to be reviewed and revised.

Table 2.5
Model Errors for Ammonia in the San Joaquin River

Monitoring Station	Relative Error	Absolute Error
Lander Avenue (Stevinson)	1.8%	6.7%
Crows Landing	135%	145%
Vernalis	48%	73%

Nitrate

Figure 2.23 through Figure 2.25 compare the time series of predicted and observed nitrate concentration. The figures demonstrate that the range of the simulations is generally within the range of the observations, an improvement over the ammonia calibration, however some seasonal errors are present. In particular at both Crows Landing and Vernalis, summer simulations are too low and winter simulations are too high.

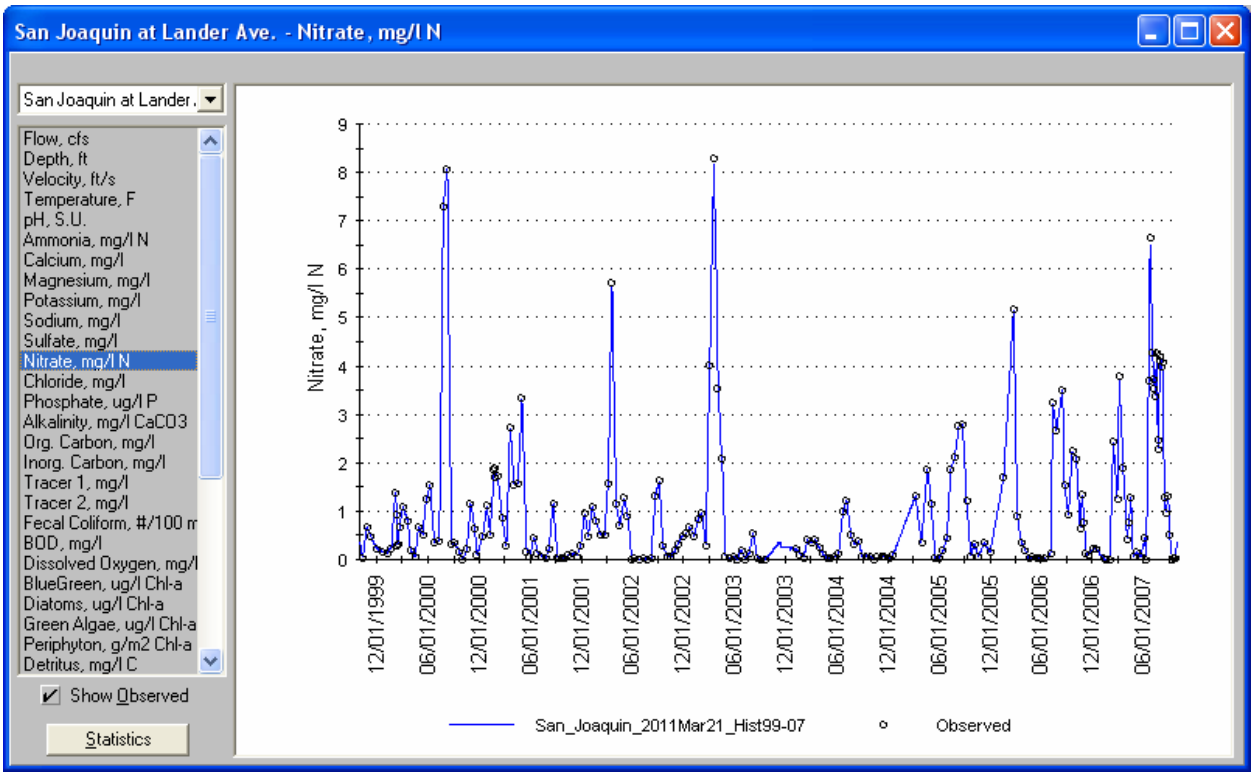

Figure 2.23 Simulated vs Observed Nitrate at Lander Avenue

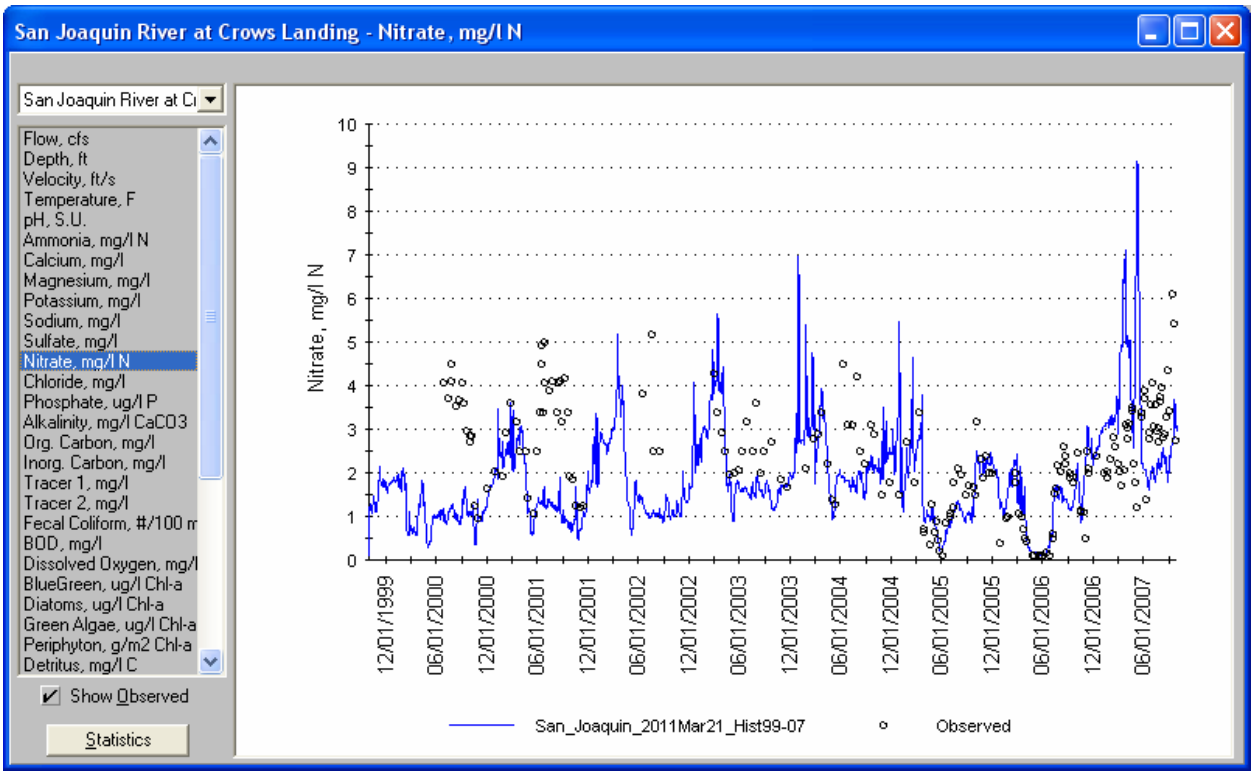

Figure 2.24 Simulated vs Observed Nitrate at Crows Landing

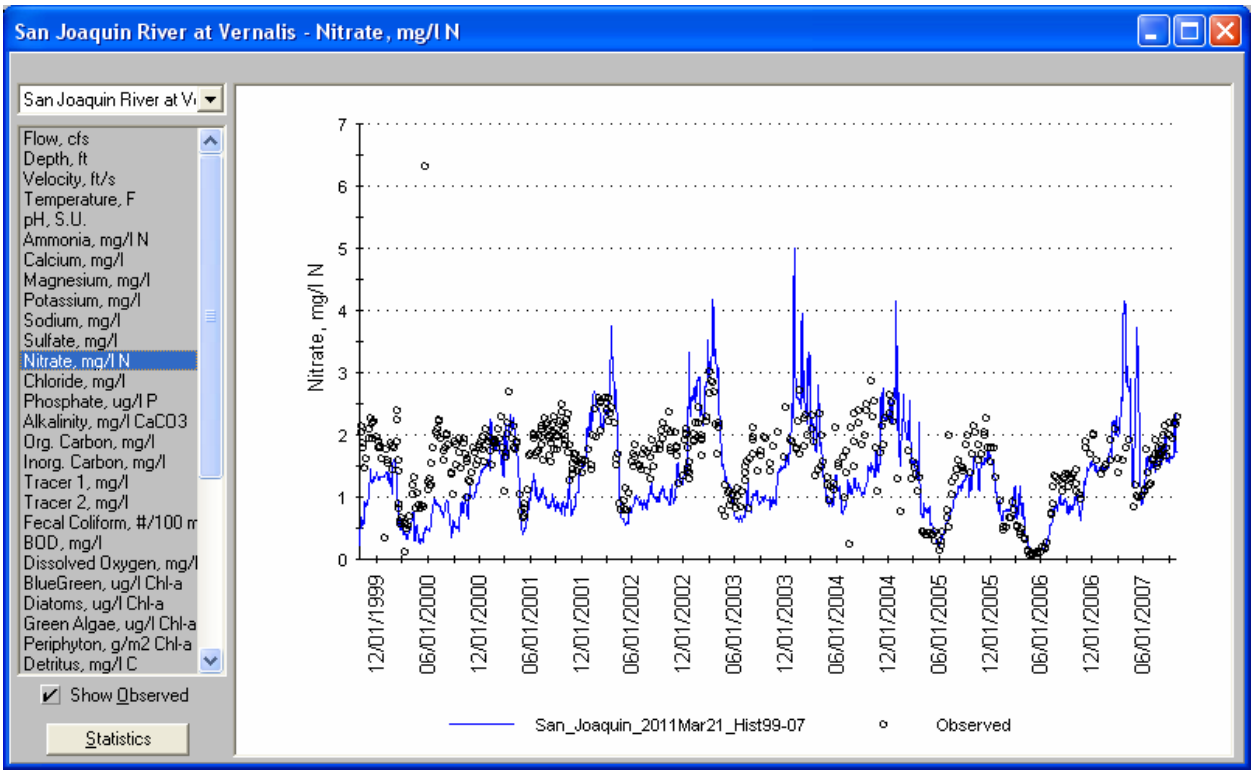

Figure 2.25 Simulated vs Observed Nitrate at Vernalis

Table 2.6 shows the model errors for nitrate at the three presented monitoring locations along the San Joaquin River. Like for other constituents, the error is low at Lander Avenue, indicating that the upstream boundary inflow is not a major source of error in the simulation further downstream. The under-simulation during summer months is causing the negative bias reflected in the relative errors at Crows Landing and Vernalis. Agricultural nonpoint sources constitute 46% of the nitrate load at Vernalis. The remaining load comes primarily from boundary inflows at 40%. Boundary inflow concentrations are based on observed data and involve significantly less uncertainty in the San Joaquin Valley than do estimates of irrigation and fertilizer application rates on agricultural land. As evidence to this, the relative error in the nitrate simulations downstream of Stanislaus, Tuolumne, and Merced boundary inflows are 0.7%, -0.4%, and 4.0%, respectively. Thus, errors in agricultural nonpoint source loads are the main cause of overall nitrate simulation errors. This is further supported by the fact that the errors are most pronounced during the summer months, when agricultural drainage dominates the flow. In order to improve the summer nitrate simulations, assumptions regarding irrigation and fertilization practices would need to be reviewed and revised.

Table 2.6
Model Errors for Nitrate in the San Joaquin River

Monitoring Station	Relative Error	Absolute Error
Lander Avenue (Stevinson)	0.8%	2.9%
Crows Landing	-27%	62%
Vernalis	-22%	40%

Total Phosphorus

24 through 26 compare the time series of predicted and observed total phosphorus concentration. Similar to nitrate, the simulations are within the range of the observed data. The pattern of the simulations matches that of the observed with higher concentrations in the summer than winter. However, the simulations are consistently too low compared to observed data.

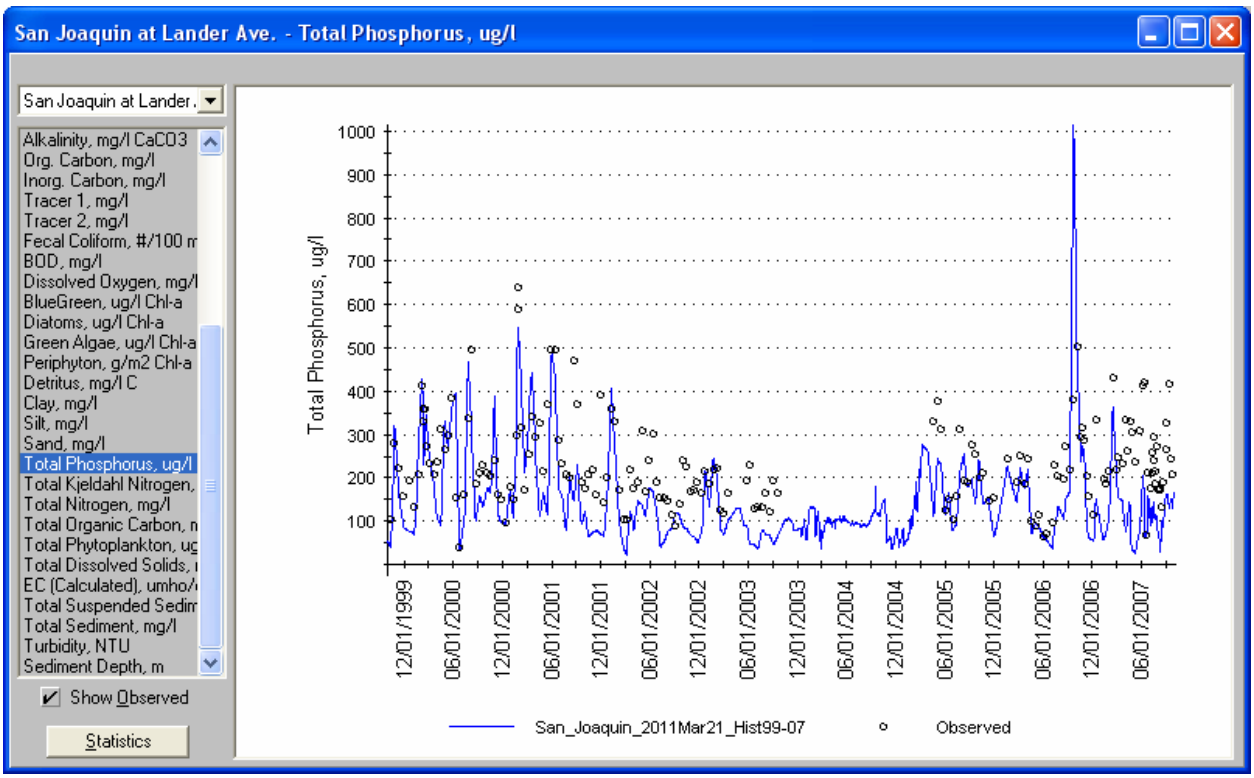

Figure 2.26 Simulated vs Observed Total Phosphorus at Lander Avenue

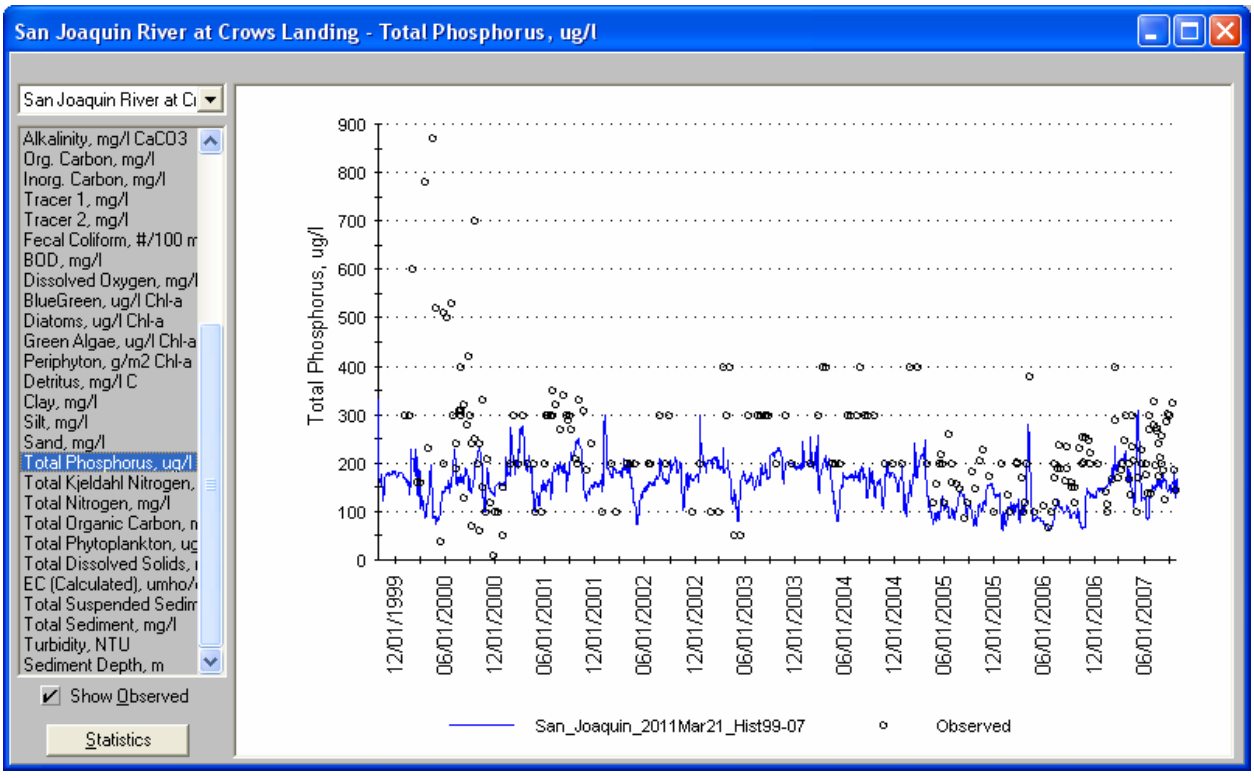

Figure 2.27 Simulated vs Observed Total Phosphorus at Crows Landing

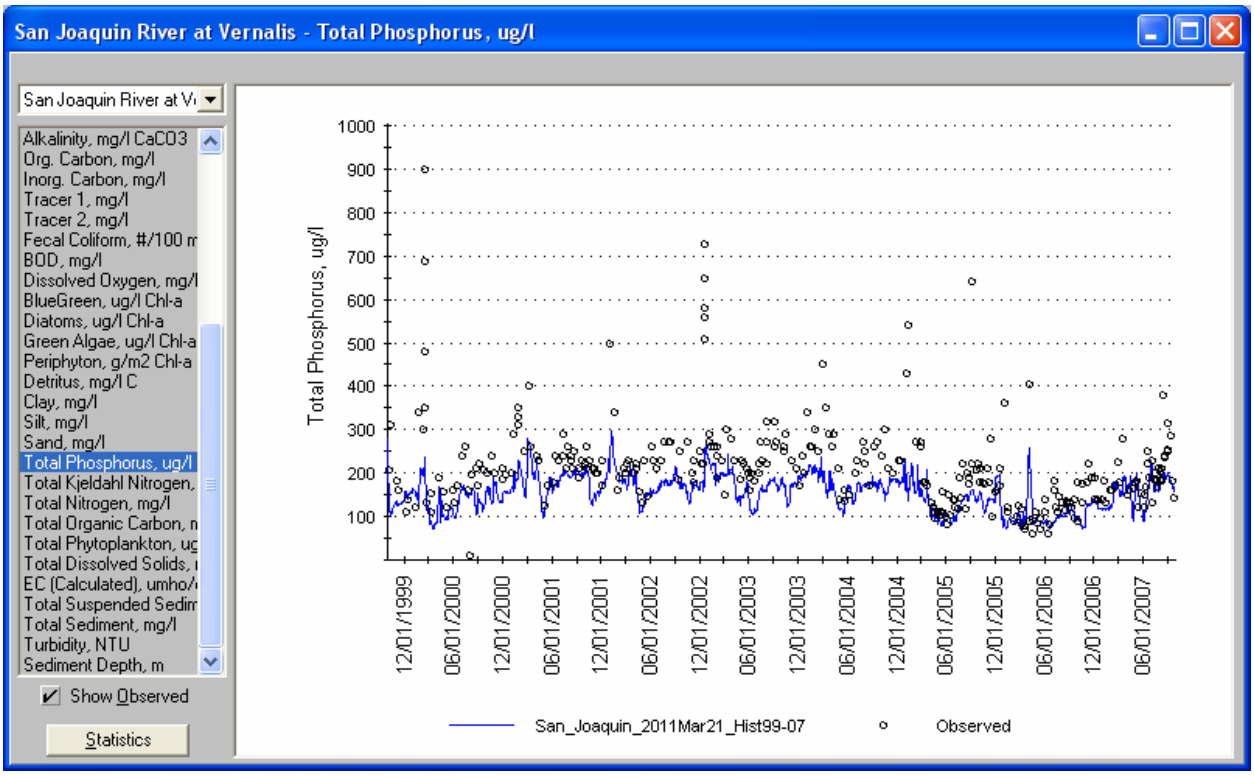

Figure 2.28 Simulated vs Observed Total Phosphorus at Vernalis

Table 2.7 shows the model errors for total phosphorus at the three presented monitoring locations along the San Joaquin River. All three monitoring locations show approximately 30% less phosphorus than observed, implying a systematic error. Boundary inflows are 23% of the total phosphorus load, point sources are 20%, scour from the river bed is 30%, and the remainder is point sources. Potential sources of error again include incorrect assumptions about agricultural practices (e.g. irrigation and fertilization) and incorrect assumptions regarding sediment adsorption and river bed / water column interactions.

Table 2.7
Model Errors for Phosphate in the San Joaquin River

Monitoring Station	Relative Error	Absolute Error
Lander Avenue (Stevinson)	-30%	40%
Crows Landing	-34%	42%
Vernalis	-28%	31%

Summary

This report focuses on model updates made to the San Joaquin River WARMF application for this project and the subsequent re-evaluation of the calibration of flow, TDS/EC, organic carbon, and nutrients. The primary updates made to the model include reclassifying catchment land use,

redefining associated land use parameters, including fertilizer application rates, and reallocating irrigation water based on the new land use classifications.

The flow calibration results at the three selected locations along the San Joaquin River (Lander Avenue, Crows Landing and Vernalis), were generally very good, with low relative and absolute errors. Since a good flow calibration is a prerequisite for a good water quality calibration, the hydrologic simulations in the San Joaquin River provided the necessary basis for obtaining reasonable water quality simulations.

The water quality parameters of concern to the Drinking Water Policy Work Group include TDS/EC, organic carbon and nutrients. Calibration results were presented and discussed for these parameters. For simulations of EC, the model did well predicting the seasonal pattern though a positive bias was introduced between Lander Avenue and Crows Landing. Since EC is a largely conservative species, the errors are likely due to assumptions regarding model inputs such as irrigation practices and fertilizer application rates.

Overall the organic carbon calibration was good with errors below the typical target maximum percentages. However, two apparent errors in simulation results of organic carbon were noted and investigated. The first was a failure of the model to predict winter peak concentrations of both dissolved and total organic carbon observed in the water quality data. The error does not appear to be caused by the model underestimating storm water runoff from urbanized areas. There could be a flushing effect from increasing flows collecting organic matter from the riparian zone or the source of the organic carbon could originate in the boundary inflows. There is insufficient data to explain the error. The second discrepancy in organic carbon simulation was the model's prediction of summer peaks of total organic carbon in 2000-2002 which were not observed in water quality monitoring data. This error was attributed to the overestimation of phytoplankton (a component of organic carbon) during the summer season due to modeling on a daily versus hourly time step.

The nutrient calibration results presented included ammonia, nitrate and total phosphorus. While the range of simulations for nitrate and phosphate were reasonable, ammonia was significantly overpredicted downstream of Lander Avenue. Based on the relative sources of ammonia in the watershed, the main source of error for ammonia is suggested as land application rates in areas of dairy land use. Errors during summer months in both the nitrate and phosphorus simulations are also likely due in large part to assumptions regarding agricultural practices. Thus to improve nutrient simulations, such assumptions would need to be re-evaluated and revised.

3 SOURCE CONTRIBUTION

Introduction

The water quality calibration in Chapter 2 is useful for checking simulations against observed data. The model also provides information about source contribution of pollutants useful to the understanding of watershed system behaviors and important to the formulation of management alternatives. WARMF keeps track of not only pollutant mass, but also its source. The sources include upstream inflows at the boundary of the model domain, point sources, and nonpoint sources identified by land use. The model calibration section of this report discussed sources of error, especially in the estimation of agricultural model inputs. These errors are reflected in the source contribution analysis. An underprediction of in-stream concentration caused by too little loading from agricultural lands, for example, will lead to an underestimate of the agricultural source contribution.

Sources of Total Dissolved Solids

The concentration of total dissolved solids (TDS) at Vernalis is a marker indicative of salty agricultural surface and subsurface drainage entering the San Joaquin River. TDS is highly correlated to electrical conductivity, which is easily measured and used to estimate the sources of TDS.

Table 3.1 summarizes the fluxes of TDS load to the San Joaquin River over the 2000 through 2007 water years as simulated by WARMF. Inflows to the model domain from tributaries accounted for 21% of the TDS inputs. 77% of the inputs came from nonpoint sources (groundwater accretion and surface runoff), primarily from agricultural land. Point sources contributed 2% of the inputs. There was a 10% net loss of salt from in-stream processes and diversions.

Table 3.1 Sources of Total Dissolved Solids to the San Joaquin River

Sources	Load (tons/day)	Load (% of inputs)
Inflows from Upstream	**769**	**21.3%**
Stanislaus River	277	7.7%
Tuolumne River	217	6.0%
Merced River	115	3.2%
San Joaquin River at Lander Ave	160	4.4%
Nonpoint Sources	***2769***	**76.7%**
Natural Land Cover	244	6.8%
Agriculture	2469	68.4%
Urban Areas	56	1.5%
Point Sources	**71**	**2.0%**
In-stream Losses and Gains*	**-364**	
NET LOAD TO THE DELTA	**3245**	

* Includes uptake, adsorption, settling, resuspension, reactions, diversions, and return flows

Figure 3.1 shows the relationship between TDS load and TDS concentration at Vernalis. High TDS loads led to high TDS concentration in the receiving water. From midsummer through midwinter, the TDS concentration increased with higher TDS loads from agricultural drainage, Mud Slough, and Salt Slough. The concentration generally increased as flow from the east side tributaries decreased. In the spring, the TDS load to the San Joaquin River was relatively low while flow was high, producing the lowest seasonal TDS concentrations.

The relationship between TDS loads and TDS concentration was unusual in the wet years of 2005 and 2006. Both TDS load and TDS concentration were dominated by the boundary river inflows in late winter and early spring. Although the load was high, the TDS concentration was lower than in a normal year.

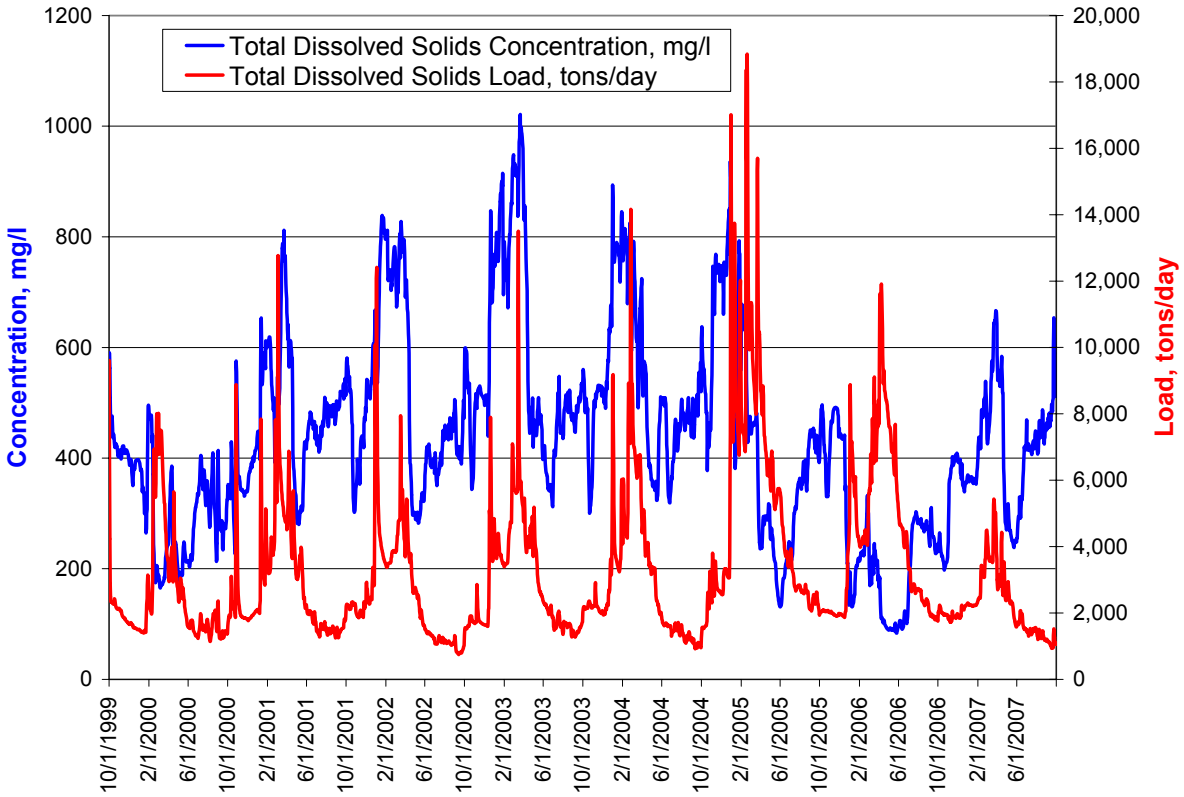

Figure 3.1 TDS Load (red line) vs. Concentration (blue line) at Vernalis

Sources of Total Organic Carbon

Table 3.2 summarizes the sources of total organic carbon load to the San Joaquin River. The tributary inflows contributed 62% of the total organic carbon loaded to the San Joaquin River, while 34% was contributed by nonpoint source load from the land. Net in-stream gains and losses nearly balanced themselves out. Point sources contributed 4% of the organic carbon load.

Figure 3.2 shows the relationship between total organic carbon load and concentration at Vernalis. Spring runoff after wet winters produced the highest loading of organic carbon. Although total organic concentrations were typically elevated in summer, the load was not elevated since this is the low flow season.

Table 3.2 Sources of Total Organic Carbon to the San Joaquin River

Sources	Load (tons/day)	Load (% of inputs)
Inflows from Upstream	**30.63**	**61.9%**
Stanislaus River	10.68	21.6%
Tuolumne River	7.36	14.9%
Merced River	4.77	9.6%
San Joaquin River at Lander Ave	7.82	15.8%
Nonpoint Sources	***16.78***	**33.9%**
Natural Land Cover	3.69	7.5%
Agriculture	12.78	25.8%
Urban Areas	0.31	0.6%
Point Sources	**2.08**	**4.2%**
In-stream Losses and Gains*	**-0.21**	
NET LOAD TO THE DELTA	**49.28**	

* Includes uptake, adsorption, settling, resuspension, reactions, diversions, and return flows

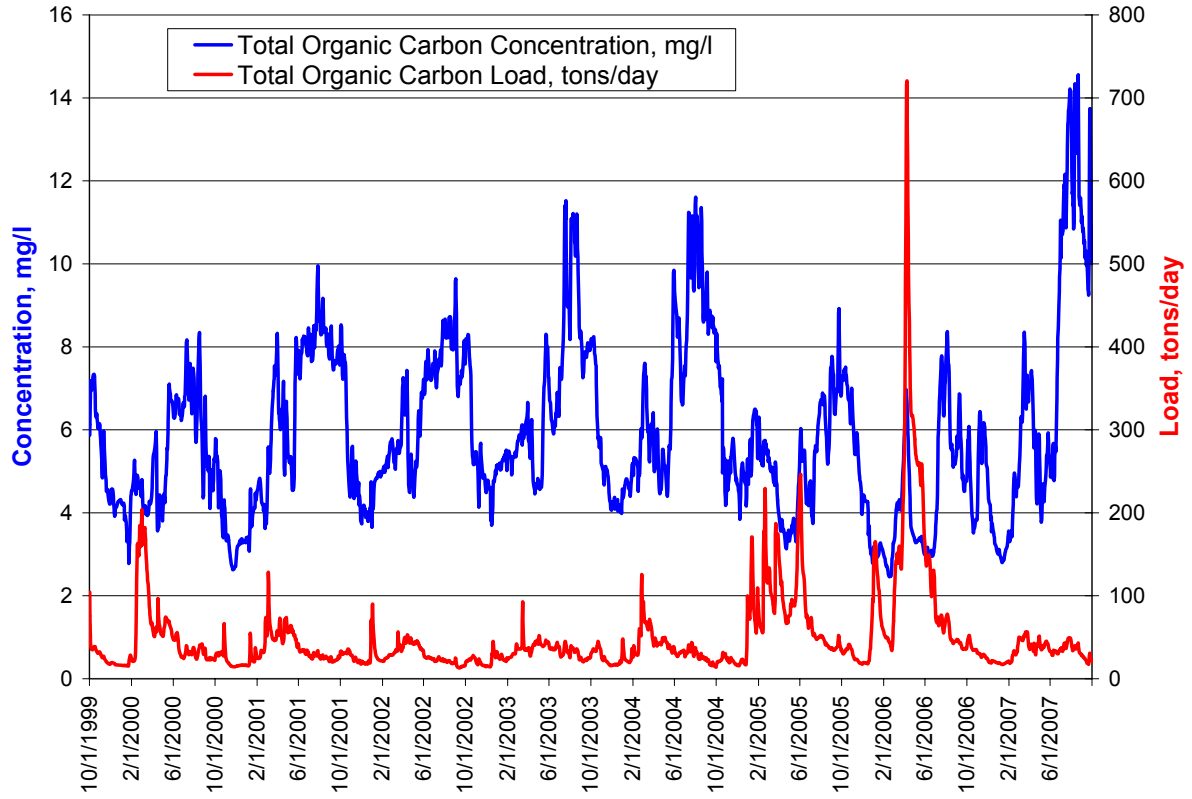

Figure 3.2 Total Organic Carbon Load (red line) vs. Concentration (blue line) at Vernalis

Sources of Nutrients

Table 3.3 summarizes the sources of total ammonia (dissolved + adsorbed) load to the San Joaquin River. The model boundary inflows contributed 21% of the ammonia loaded to the San Joaquin River, while 75% was contributed by nonpoint source load from the land, primarily dairies. Point sources contributed 4% of the ammonia load. A net in-stream loss (including nitrification, settling, and uptake by phytoplankton) was responsible for removal of 48% of the ammonia load.

Table 3.3 Sources of Total Ammonia to the San Joaquin River

Sources	Load (tons/day)	Load (% of inputs)
Inflows from Upstream	**1.28**	**21.2%**
Stanislaus River	0.3	5.0%
Tuolumne River	0.22	3.6%
Merced River	0.64	10.6%
San Joaquin River at Lander Ave	0.12	2.0%
Nonpoint Sources	***4.51***	**74.5%**
Natural Land Cover	0.12	2.0%
Agriculture	4.28	70.7%
Urban Areas	0.10	1.7%
Point Sources	**0.27**	**4.4%**
In-stream Losses and Gains*	**-2.89**	
NET LOAD TO THE DELTA	**3.16**	

- Includes uptake, adsorption, settling, resuspension, reactions, diversions, and return flows

Figure 3.3 shows the relationship between concentration and load of total ammonia. The two curves diverge when flow is very high and suspended sediment carries extra adsorbed ammonia.

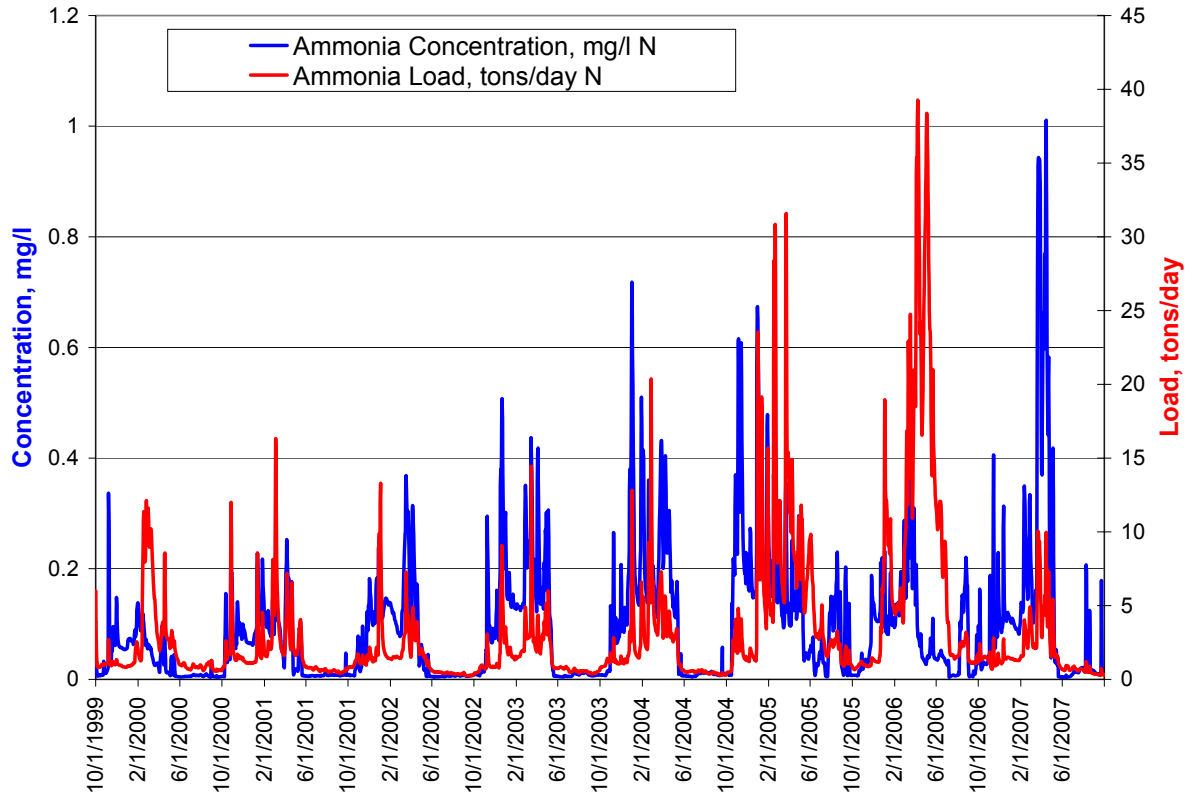

Figure 3.3 Total Ammonia Load (red line) vs. Concentration (blue line) at Vernalis

Table 3.4 summarizes the sources of nitrate load to the San Joaquin River. Model boundary inflows contributed 42% of the nitrate loaded to the San Joaquin River, while 52% was contributed by nonpoint source load from the land directly to the San Joaquin River. Point sources contributed 7% of the nitrate load. A net loss (including uptake by phytoplankton) was responsible for removing 12% of the nitrate.

Table 3.4Sources of Nitrate to the San Joaquin River

Sources	Load (tons/day)	Load (% of inputs)
Inflows from Upstream	**4.83**	**41.7%**
Stanislaus River	1.15	9.9%
Tuolumne River	1.74	15.0%
Merced River	1.53	13.2%
San Joaquin River at Lander Ave	0.41	3.5%
Nonpoint Sources	***5.98***	**51.6%**
Natural Land Cover	0.65	5.6%
Agriculture	5.25	45.3%
Urban Areas	0.07	0.6%
Point Sources	**0.78**	**6.8%**
In-stream Losses and Gains*	**-1.43**	
NET LOAD TO THE DELTA	**10.16**	

Figure 3.54 compares the nitrate load with concentration. Both the concentration and load are highest in winter and decrease in spring and summer as flow decreases. The highest loads coincide with the highest flow of the year in spring.

* Includes uptake, adsorption, settling, resuspension, reactions, diversions, and return flows

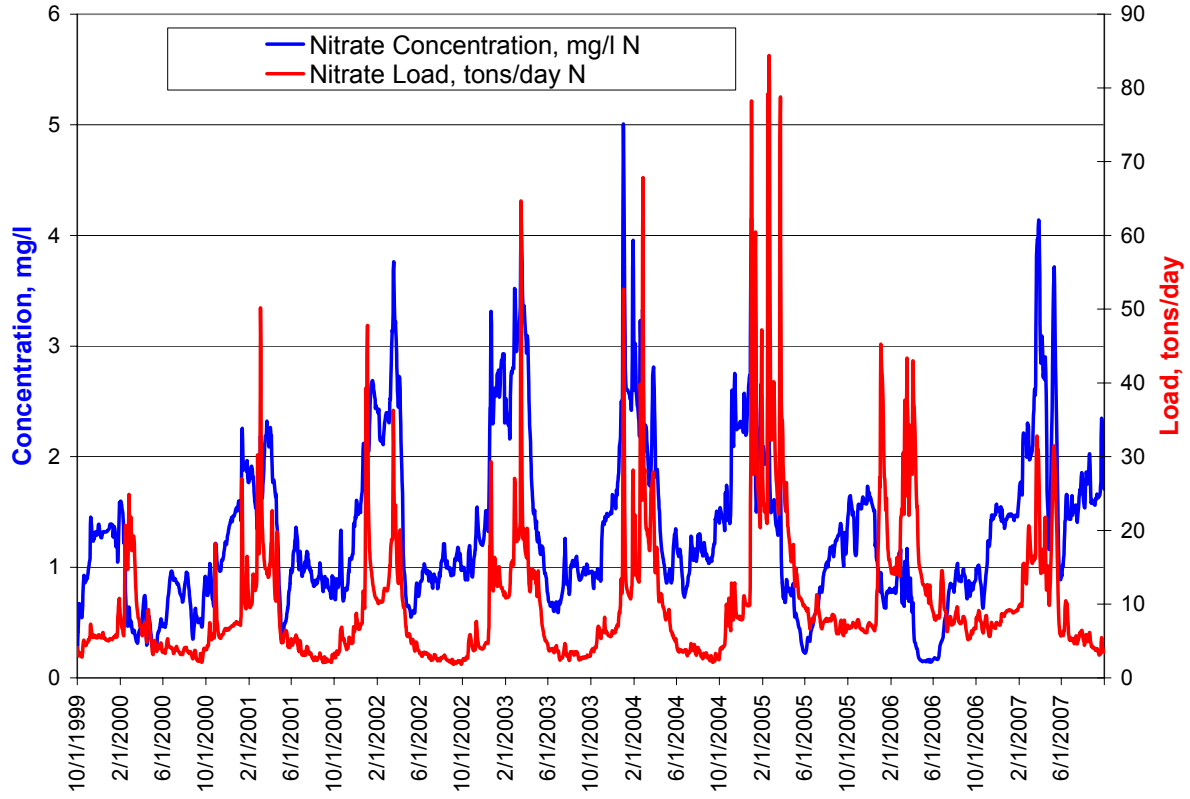

Figure 3.4 Nitrate Load (red line) vs. Concentration (blue line) at Vernalis

Table 3.5 summarizes the sources of total phosphorus load to the San Joaquin River. The tributary inflows contributed 39% of the phosphate loaded to the San Joaquin River, while 44% was contributed by nonpoint source load from the land. There was little net gain or loss in-stream. Point sources contributed 12% of the phosphate load.

Table 3.5 Sources of Phosphate to the San Joaquin River

Sources	Load (tons/day)	Load (% of inputs)
Inflows from Upstream	**0.53**	**43.7%**
Stanislaus River	0.16	13.2%
Tuolumne River	0.15	12.4%
Merced River	0.065	5.4%
San Joaquin River at Lander Ave	0.155	12.8%
Nonpoint Sources	***0.54***	**44.6%**
Natural Land Cover	0.14	11.3%
Agriculture	0.39	32.4%
Urban Areas	0.01	0.9%
Point Sources	**0.14**	**11.7%**
In-stream Losses and Gains*	**0.01**	
NET LOAD TO THE DELTA	**1.22**	

* Includes uptake, adsorption, settling, resuspension, reactions, diversions, and return flows

Figure 3.5 compares total phosphorus load with concentration. The concentration is highest in winter but decreases in spring. The highest loads coincide with the highest flow of the year in spring.

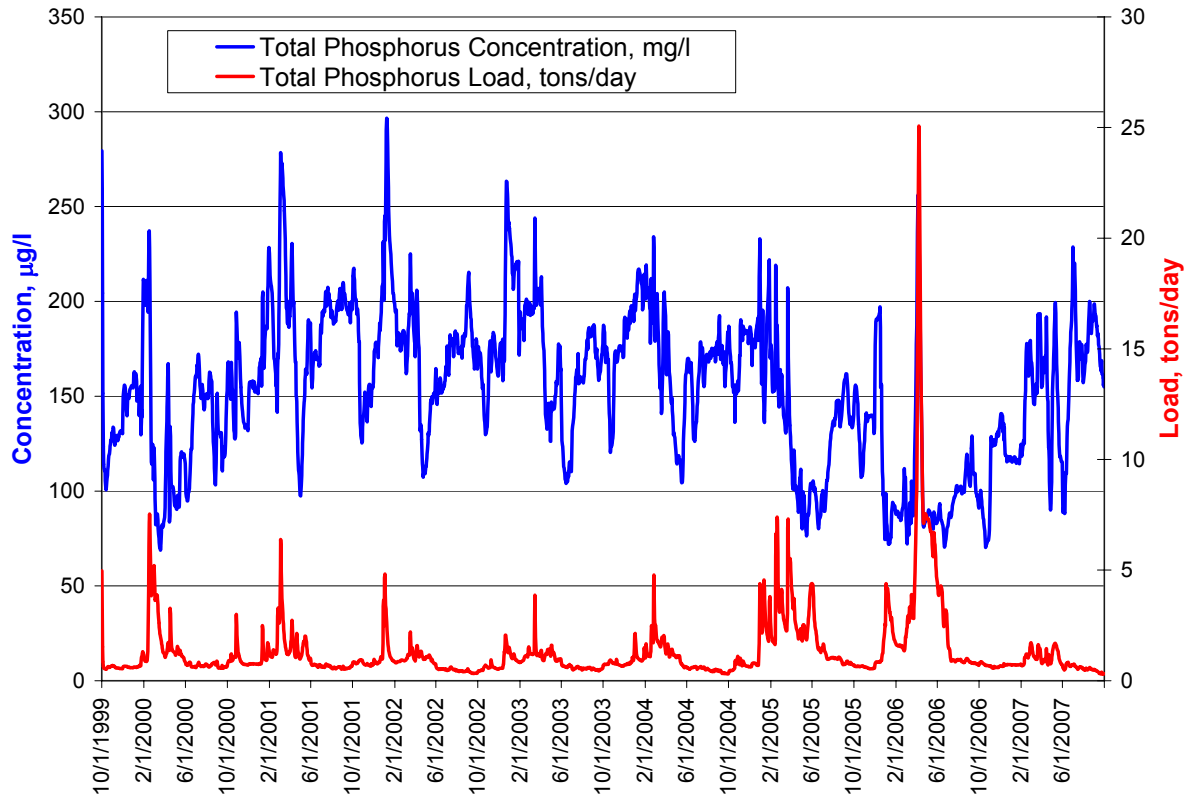

Figure 3.5 Total Phosphorus Load (red line) vs. Concentration (blue line) at Vernalis

4 CONCLUSION AND RECOMMENDATIONS

Conclusion

After updating landuse and associated model parameters, a reevaluation of the calibration of the WARMF model showed good results for flow and reasonable results for total dissolved solids / electrical conductivity, dissolved organic carbon, and total organic carbon. Larger errors were present in nutrient simulations. The model was heavily constrained by agricultural inputs including applied water rates and land application rates so that relatively little could be done by calibration to improve the match between simulation results and observed data.

Calibration of electrical conductivity did well predicting the seasonal pattern, though a positive bias was introduced due to assumptions regarding model inputs such as irrigation practices and fertilizer application rates.

Overall the organic carbon calibration was good with errors mainly below the typical target maximum percentages. However, total organic carbon simulations showed two types of systematic errors in the early part of the simulation period: a failure to simulate the winter peaks which were measured at Vernalis and simulation of summer peaks which were not measured in 2000-2002. The latter problem can be explained by the underestimation of phytoplankton due to the model's daily time step, but there are multiple possible explanations for the observed winter peaks. Since the winter peaks of organic carbon can coincide with the rising limb of the spring runoff hydrograph, targeted monitoring can evaluate whether the source of the high organic carbon concentration is the reservoirs, the east side tributaries, or the San Joaquin River proper. Measuring the dissolved and total organic carbon in the tributaries and at multiple locations in the San Joaquin River during the start of spring runoff is recommended to identify the source of the organic carbon loading.

Simulated nutrient concentrations followed the annual pattern seen in the observed data, but had errors which were probably caused by incorrect agricultural input coefficients. Nitrate and total phosphorus concentrations were generally lower than observed while ammonia was higher than observed because of a large amount of loading from dairy land application areas. Errors during summer months in both the nitrate and total phosphorus simulations are also likely due in large part to assumptions regarding agricultural practices. Thus to improve nutrient simulations, it is recommended to reevaluate and revise irrigation and land application model assumptions.

The sources of total dissolved solids were identified. About 2/3 of the TDS loading comes from the concentrated sources of groundwater accretion, Mud Slough, Salt Slough, and agricultural drains. Since TDS from groundwater and west side tributaries contribute substantial loading to the San Joaquin River, the concentration of TDS is in large part a function of the amount of fresh water from the east side tributaries is available for dilution. Control of TDS at Vernalis can be

done by changing agricultural practices which cause the TDS loading or changing the management of the east side reservoirs which dilute it.

Total organic carbon loading is not dominated by a few concentrated sources, but rather comes from a combination of groundwater accretion, tributary inflows, and in-stream generation by phytoplankton. Peak concentrations in summer caused by phytoplankton blooms occur when flow is relatively low, while winter peak concentrations occur when flow is high. Control of the seed phytoplankton entering the San Joaquin River from its tributaries can reduce the summer peak concentrations, but more needs to be learned about the cause of winter organic carbon peak concentrations before control strategies can be devised.

The sources of nutrients were predominantly the tributary inflows and nonpoint sources from the land. However nutrient simulations should be improved by revising assumptions pertaining to agricultural practices prior to formulating management strategies.

Recommendations

The model application process used relied upon extensive knowledge of agricultural processes to constrain the model. While this is very valuable information to incorporate into the model, there is uncertainty in this knowledge which can cause model error if used verbatim without additional calibration as it was in this case. The model can provide expert "knowledge" of watershed physical processes as a feedback mechanism to determine the right model parameters to use. It is recommended that continued modeling work allow for a range of possible values for model inputs which can then be adjusted through model calibration.

The first priority would be to adjust irrigation practices to improve the model's simulation of electrical conductivity / total dissolved solids. Since this is a relatively conservative parameter, a good calibration requires accurate accounting of applied water, groundwater recharge, and groundwater usage. With those model inputs adjusted, land application rates and other model parameters can be adjusted to improve model simulation of nutrients.

5 REFERENCES

Driscoll, Jr. C. T., R.A. Bodaly, O.R. Bullock, Jr., D.P. Krabbenhoft, R.P. Mason, C.D. Pollman, and T. A. Wool. 2004. "Report of The Peer Review Panel on the Development of the Watershed Analysis Risk Management Framework (WARMF) Model to Assess Mercury in the Western Lake Superior Basin, Minnesota", University of Minnesota Sea Grant Program, Duluth, Minnesota, Publication No. CT 15.

Herr, J., Weintraub, L.H.Z., and Chen, C.W. 2001. "User's Guide to WARMF: Documentation of Graphical User Interface," EPRI, Palo Alto, CA. Topical Report.

Herr, J., and C. W. Chen 2006 (a). "Calibration Report": a deliverable report for the CALFED Project ERP-02D-P63, Monitoring and Investigation of the San Joaquin River and Tributataries Related to Dissolved Oxygen, Task 6 Model Calibration and Forecasting. Systech Engineering, Inc. San Ramon, California.

Herr, J., C. W. Chen 2008. "Extension of WARMF Model of the San Joaquin River from Lander Avenue to Friant Dam (Phase I) ": a deliverable report for the Bureau of Reclamation WARMF Extension Contract. Systech Water Resources, Inc. Walnut Creek, California.

Herr, J., C. W. Chen, and K. van Werkhoven 2008. "Final Report for the Task 6 Modeling of the San Joaquin River": a deliverable report for the CALFED Project ERP-02D-P63, Monitoring and Investigation of the San Joaquin River and Tributaries Related to Dissolved Oxygen, Task 6 Model Calibration and Forecasting. Systech Water Resources, Inc. Walnut Creek, California.

Jones & Stokes. 2005. "San Joaquin River Deep Water Ship Channel Demonstration Dissolved Oxygen Aeration Facility Initial Study/Mitigated Negative Declaration". Prepared for California Department of Water Resources.

Keller A., 2000 "Peer review of the watershed analysis risk management framework (WARMF): an evaluation of WARMF for TMDL applications by independent experts using USEPA guidelines", Electric Power Research Institute, Palo Alto, CA. Technical Report 1000252.

Keller A. 2001. "Peer Review of the Acid Mine Drainage Module of the Watershed Analysis Risk Management Framework (WARMF) – An evaluation of WARMF/AMD using EPA Guidelines", Electric Power Research Institute, Palo Alto, CA. Technical Report 1005182.

Kratzer, C.R., P.D. Dileanis, C. Zamora, S. R. Silva, C. Kendall, B.A. Bergamaschi, and R. A Dahlgren. 2004. "Sources and Transport of Nutrients, Organic Carbon, and Chlorophyll-a in the

San Joaquin River Upstream of Vernalis, California, during Summer and Fall, 2000 and 2001", Water Resources Investigations Report 03-4127, US Geological Survey, Sacramento, CA.

List, E.J. and S.C. Paulsen, 2008. "Peer Review of San Joaquin River Watershed Modeling" Final Draft, Flow Science Incorporated, Pasadena, CA.

"Salt and Nitrate Sources Pilot Implementation Study Report" by Larry Walker & Associates, Luhdorff & Scalmanini Consulting Engineers, Systech, Newfields Agriculture and Environmental Resources, and the UC Davis Department of Land, Air, and Water Resources, February 2010.